Detecting geomorphic responses following invasive vegetation removal: Wickaninnish Dunes, Pacific Rim National Park Reserve, British Columbia, Canada

by

Jordan Blair Reglin Eamer
B.Sc., University of Victoria, 2010

A Thesis Submitted in Partial Fulfillment of the
Requirements for the Degree of

MASTER OF SCIENCE

In the Department of Geography

Detecting geomorphic responses following invasive vegetation removal: Wickaninnish Dunes, Pacific Rim National Park Reserve, British Columbia, Canada

by

Jordan Blair Reglin Eamer
B.Sc., University of Victoria, 2010

Supervisory Committee

Dr. Ian J. Walker, Department of Geography
Supervisor

Dr. K.O. Niemann, Department of Geography
Departmental Member

Supervisory Committee

Dr. Ian J. Walker, Department of Geography
Supervisor

Dr. K.O. Niemann, Department of Geography
Departmental Member

Abstract

This thesis presents results from a large-scale dynamic restoration program implemented by Parks Canada Agency (PCA) to remove invasive marram grasses (*Ammophila* spp.) from a foredune-transgressive dune complex in Pacific Rim National Park, British Columbia, Canada. The program goal is to restore habitat for endangered Pink sandverbena (*Abronia umbellate var breviflora*) as required by the Canadian Species at Risk Act (SARA). Three sites were restored by PCA via mechanical removal of invasive marram grasses (*Ammophila spp.)* in September 2009. This study documents geomorphic and sediment mass exchange responses at one of these sites as derived from detailed Digital Elevation Model (DEM) surveys of a 10 320 m^2 study area that spans three discrete geomorphic units (beach, foredune, and transgressive dune complex). Subsequent approximately bi-monthly total station surveys for the first year post-restoration are compared to a pre-restoration baseline Light Detection and Ranging (LiDAR) survey (August 2009) to quantify and describe morphodynamic responses and volumetric changes. Two different methodologies were utilized for post processing of volumetric change DEMs in order to filter out non-statistically significant change. The first filter used software developed for fluvial geomorphology and was tested using the student's *t* distribution. This approach, while novel in the field of coastal geomorphology, was less complex than the second which was based on spatial statistical procedures

popular in the ecological sciences. This filter was based on local Moran's I_i, which was used to generate 1.5m and 5m distance thresholds of statistically significant geomorphic change. These thresholds were specified to simulate the outer limit of saltating grains and the dimensions of landform development, respectively. Results show that the beach receives appreciable sediment supply via bar welding and berm development in the winter, much of which is transported to the foredune and transgressive dune complex units in the spring. This promotes rapid redevelopment of incipient dunes in the backshore, rebuilding of the seaward slope of the foredune following wave scarping, and localized extension of depositional lobes in the transgressive dune complex fed by sediment from the beach and foredune stoss (only shown in local Moran's I_i results). The results of this study suggest that the foredune-transgressive dune complex at Wickaninnish Dunes has experienced enhanced aeolian activity and positive sediment volume changes over the first year following mechanical restoration. In addition, comparison of the two methodologies show that spatial statistics were found to provide both more realistic calculated volumes at a smaller threshold distance (e.g., $-0.012 m^3 m^{-2}$ in the foredune after devegetation; only $+0.015 m^3 m^{-2}$ in the transgressive dune complex in the year following restoration) and better highlighting of important spatial processes at a larger threshold distance (e.g., foredune stoss erosion; feature highlighting) than the volumetric change calculations based on a simpler statistical threshold.

Contents

List of Figures

List of Tables

Acknowledgements

A big thank you to my supervisor, Ian Walker, for his guidance and motivation through these last two years. Thank you to my committee member, Olaf Niemann for opportunities in his lab and general LiDAR prowess.

To my labmates, past and present, thanks for keeping me sane! You know who you are HERB, DK, (Dr.) Darke, CC, KA, NvW.

To my brother, mom, and dad, thanks for believing!

To my partner JL, thanks so, so much for your support.

To my little boy, Tyler…

let's go on vacation!

1. Introduction

1.1. Research Context

1.1.1. Coastal dune morphodynamics

Aeolian (windblown) sediment transport is a key component to coastal geomorphology, and associated dune formation is a function of the volume of available sand on the beach, the shape and width of the beach, and the nature of the wind regime (i.e., frequency, magnitude and directionality) (Short and Hesp, 1982; Psuty, 2004). Vegetation and other roughness elements (e.g., large woody debris) in the backshore trap sand allowing for the formation and growth of foredunes (Hesp, 2002; Eamer and Walker, 2010). Beach-dune dynamics are a key factor in the classification of beaches (Short and Hesp, 1982). Incoming wave energy (high, moderate, low) is directly related to beach form (dissipative, intermediate, reflective) and geomorphology landward (large-scale transgressive dune complexes and large stable foredunes, isolated parabolic dunes and blowouts with moderate and unstable foredunes, minimal landward aeolian deposition with small foredunes). The wind regime ultimately controls beach-dune dynamics, sediment transport beyond the backshore and develop established foredunes, and the size of the dune (Short and Hesp, 1982), and greater onshore wind velocity increases the potential for sediment transport to the backshore and foredunes. Sediment availability is one of the dominating variables that drives the development of the foredune characteristics, though it regularly depends on the transporting availability of the waves (Hesp, 2002; Psuty, 2004). Additional factors controlling dune development include: (i) sand supply; (ii) vegetation characteristics; (iii) rate of aeolian sand accretion

and/or erosion; (iv) charactertics of transporting winds; (v) the occurrence and magnitude of storm erosion, dune scarping, and overwash processes; (vi) medium to long term beach or barrier state; (vi) sea/lake/estuary water level; (vii) extent of human impact and use (Hesp, 2002)

Improved understanding of coastal dune dynamics is important in light of ongoing and future impacts of climate change and sea level rise. As eustatic sea level appears to be rising in many areas at about 1-2 mm/y over the past century (Gornitz, 1995), coastal scientists are tasked with providing reasonable scenarios for the effects of sea-level rise on coastal processes and shoreline position (Davidson-Arnott, 2005). The *de-facto* standard for half a century was the Bruun Model (Bruun, 1954), which is constructed from three hypotheses resulting from an increase in sea-level (Bruun, 1962): i) wave erosion erodes the upper beach, ii) the exact volume of material from the upper beach is deposited in the nearshore, and iii) the thickness of nearshore deposition is equivalent to the amount of sea-level rise. While this served the purposes of the time, understanding of backshore dynamics and the relationship between beach and dune sediment budgets (e.g., Nickling and Davidson-Arnott, 1990; Psuty, 1988; Sherman and Bauer, 1993), along with the complete disregard for coastal dune sediment budget inherent in the Bruun Model, led to a conceptual re-evaluation by Davidson-Arnott (2005). In this model, termed the RDA model, three key components are discussed: i) the beach and foredune are eroded as a result of sea level rise, and the beach-dune interface migrates shore- and upward, ii) nearshore migration of sediment keeps pace with rising sea level, and iii) all sediment eroded from the dune is transferred landward, resulting in landward migration of the foredune and no net loss of sediment from the dune. Better understanding of foredunes as

dynamic features in the event of sea-level change is warranted as they often act as important buffers for shore-proximal ecosystems and coastal towns to coastal erosion, storm surges, and gradual sea level rise.

Coastal dune systems are the manifestation of a suite of processes and sedimentary responses that are difficult to model, ergo studies typically adopt one of three perspectives: i) beginning at the micro scale, with the investigation of sediment entrainment and boundary layer airflow; ii) beginning at the macro-scale, looking at a beach-dune system or dunefield and reconstructing the environmental history of the system; iii) the emerging approach of confining the study to the meso-scale, with data collection spanning longer temporal scales and the increasing use of digital elevation models (DEMs) to represent process-response dynamics. Despite advances in these three areas, the field has suffered from difficulties in bridging the scales, as the three approaches are conceptually and methodologically incompatible (Sherman, 1995).

1.1.2. Technological advances in characterizing coastal dunes

Given the broad spatial and temporal scales the field of geomorphology operates in, advances in knowledge often correspond with advancements in methods of data collection and management. The advent of airborne Light Detection and Ranging (LIDAR) has opened up new insights into meso- and macro-scale surface dynamics. Recent studies have used LIDAR in evaluating climate change impacts due to sea level rise (e.g., Webster et al., 2006), monitoring beach nourishment (e.g., Gares et al., 2006), and environmental reconstruction of a coastal system to assess response to sea-level change (e.g., Wolfe et al., 2008). Brock et al. (2002) show how LIDAR can be used for

the regional mapping of geomorphic change along sandy coasts in the United States, particularly in response to storms or long-term sedimentary processes such as coast progradation. Sallenger et al. (2003) used airborne topographic LIDAR to quantify beach topography and change along the North Carolina coast. Using LIDAR data to quantify volumetric changes in coastal systems is gaining momentum (e.g., Woolard and Colby, 2002; Zhang et al., 2005), however issues with how this relatively new data-collection method in the generation of DEMs must be taken into account (Liu, 2008). LIDAR is also an extremely powerful tool when combined with other remote sensing techniques such as with multi- or hyperspectral images for the classification of coastal land covers (e.g., Lee and Shan, 2003) or studying beach morphodynamics (e.g., Debruyn et al., 2006).

Interpolation, defined as reconstruction of the underlying continuous field of data from the limited evidence of the control points (O'Sullivan and Unwin, 2003), is of growing importance in the quantitative aspects of the natural sciences. It has existed for decades, flourishing with the advent of Geographic Information Systems in the 1960's, and traditionally has relied on deterministic methods such as proximity polygons, local spatial average, nearest neighbour, inverse-distance weighted spatial average, Triangulated Irregular Network (TIN), and spline fitting (O'Sullivan and Unwin, 2003). Of these, only nearest neighbour (when the data density is sufficiently high, such as in Light Detection and Ranging (LIDAR) datasets (Liu, 2008)) and spline fitting (e.g., Mitasova et al., 2005) are still commonly used in coastal analysis.

In a general sense, these surfaces can be approximated by letting the data speak for itself by application of regression methods to spatial coordinates, termed trend surface

analysis (O'Sullivan and Unwin, 2003). The results from this analysis can be thought of as a first-order trend in the data, as it is often a linear trend surface (plane). What differentiates this method from those previously mentioned is that the surface is generated as a best-fit to the data, is not an *exact interpolator* (doesn't honour all datapoints), and as such outputs residuals from which the square of the coefficient off multiple correlation (R^2) can be calculated. Ergo this is the first interpolation method that allows us to assess how well the model performed in interpolating the surface. Trend surface analysis, however, is not without it's shortfalls: i) there is generally no reason to assume that the attribute under analysis varies in such a simple way, ii) not all control points are honoured, and iii) there is essentially no analyst input into the selection of the trend surface model.

The decline in popularity of the aforementioned exact interpolator methods is largely due to realization that there is a degree of arbitrariness in the choice of interpolation algorithm parameters. For example, a typical approach with nearest neighbour is to use trial and error to determine the number of neighbours to average—or as with spline fitting, the smoothing and tension—with qualitative assessment of the generated surface deemed sufficient to select one and reject another. The methodology, while often “expert-driven”, does not refer to the characteristics of the data itself. Conversely, trend surface analysis, while letting the data speak for itself, doesn't allow for much (if any) “expert-driven” analysis, as it essentially regresses a surface to the data. Ideally, there should be a interpolator that allows for both the characteristics of the data and the knowledge that the analyst can offer. Krige (1951) devised a series of empirical methods that would later become the basis for a suite of geostatistical interpolators

known as Kriging that was developed into a theoretical framework by Georges Matheron (Agterberg, 2004). Kriging is considered an *optimal* (makes best use of what can be inferred about the spatial structure of the surface) *statistical* (allows for the data to speak for itself) *interpolator* (O'Sullivan and Unwin, 2003). In the simplest terms, it is the combination of a distance-weighted method and trend surface analysis. It has only recently been applied to the coastal sciences (e.g Swales, 2002; Woolard and Colby, 2002; Zhang et al., 2005). The basic principles of Kriging, and how they combine to generate an optimal interpolator for coastal surfaces, is explained in Swales (2002). While this study was confined to the beach setting, and did not extend past the backshore, there were nevertheless valuable conclusions drawn, such as: i) de-trending the data via trend surface analysis to satisfy the stationarity assumption (Goodman, 1983; Unwin, 1975) is an integral (and oft-forgotten) step, ii) experimental variograms display a high degree of spatial continuity, and thus should be well approximated, whether by some form of least-squares criteria, by trial and error (i.e., using cross-validation (Swales, 2002)), or from expert-driven approaches (Englund and Sparks, 1991), iii) short-term changes in beach surface are more difficult to model significantly in periods of accretion rather than periods of erosion, due to magnitude differences in the surface change, and iv) an ideal methodology, rather than interpolating between profiles as was done by the author, is to monitor a beach segment with an array of points.

1.1.3. Coastal dune restoration

Coastal and inland dunes have historically been subject to intense stabilization efforts (e.g., Rozé and Lemauviel, 2004) to reduce wind erosion and sand drift (Grootjans et al., 2002). Recently, more dynamic coastal restoration approaches that increase natural

geomorphic processes are utilized to provide more resilient landforms and, thus, more favourable ecological conditions for native species (Nordstrom, 2008). As this is a recent policy shift in only a few countries (the Netherlands (e.g., van Boxel et al., 1997; Arens et al., 2004), New Zealand (Hilton, 2006), and the United States (e.g., Van Hook, 1985) for example), there are few examples in the literature of documented dynamic coastal restoration projects.

One example of a recent effort in restoring dynamism is provided by van Boxel et al. (1997), for which several blowouts on the Dutch coast were re-activated and the blowout morphology, vegetation dynamics, and lime content (i.e., Potential nutrients) were monitored. Largely an ecological paper, the results from the three years of monitoring indicated that:

1. The influence of relative humidity associated with weather systems on morphological changes is great. For example, in the study site, although easterly winds are less frequent and weaker than westerlies, morphology is dominated by them due to the fact that they are associated with a low relative humidity and precipitation,
2. The mosses in the study area tolerated little to no burial, whereas marram grass was able to establish right in the blowout, and
3. Lime content was highest in the blowout, with diminished (but remaining) lime in the depositional lobes. Marram grass and mosses contribute to soil acidification.

Finally, the authors conclude that most of the small blowouts re-stabilized, whereas the medium sized blowouts actually grew in area. The authors confirm that the marram grass does not suffer from burial at all, actually requiring it for survival.

Arens et al. (2005) provides an account of a Dutch restoration of dune mobility at three study sites. This paper shifts focus from documenting ecologic to geomorphic response, using airphoto analysis for two of three sites (monitoring re-stabilization after mechanical re-activiation) and summarizing results from Arens el al. (2004) for the third site, which was much more extensively monitored using aerial photography, erosion pins, and climate data analysis. Results showed a massive initial increase in aeolian activity, with large vegetated areas invaded by sand and changing the vegetation dynamics of the area. Deflation of the newly erodible sand led to a reduction in surface elevation, and after five years significant portions of the dunes were re-stabilizing with vegetation, outpacing naturally occurring newly activated areas. To achieve durable dune mobility, the sand must remain active, whether by permanent or recurring disturbances or by the presence of high-easily erodible dunes.

A more recent study in dynamic restoration was undertaken by Kollmann et al. (2009). It involved mechanical removal of an invasive shrub from the coastal dunes of Denmark. While some geomorphic information was taken in the vegetation mapping process (i.e., identification of geomorphic unit, slope, and aspect), this study, similar to the van Boxel et al. (1997) study, was concerned with documenting the ecological response to restoration. Relative findings indicate that mechanical removal was not sufficient for fully preventing re-sprouting of remaining vegetation fragments, and the authors indicate that this is not unlike other results (e.g., D'Antonio and Meyerson, 2002).

Also, they recommend burial-enhancing structures (such as sand fences) over the restored area to assist in preventing re-sprouts.

1.1.4. Research gap

The current state of coastal studies at the meso-scale is clearly lacking from at least one of: proper characterization of the geostatistics involved in the study, an appropriate interpolation method, an appropriate sampling method, a proper description of error, and/or integration of that error into results to determine significant changes. To date, a coastal study with properly reported geostatistics has not been documented using the array of data recommended in Swales (2002). Nor has the realization that separation into geomorphic units (beach, foredune, and transgressive dune complex) should drastically decrease interpolation error, as they all exhibit drastically different underlying trends due to the processes involved (swash dominated sediment transport, topographic steering (Walker et al., 2006), and alignment to dominant wind direction (e.g., Arens, 2004; Martinho et al., 2010)) that are important to remove (Swales, 2002). Finally, proper characterization of the geomorphic response of a coastal *system* to dynamic coastal restoration hasn't been attempted, or reported in the literature, to date.

To reiterate Sherman (1995), the key to bridging the different scales of coastal processes is at the meso-scale, and require proper characterization of surface change to be correlated with process-based as well as environmental change assessment. Elaborating upon that, Bauer and Sherman (1999) identify one of the two most pressing needs facing the coastal aeolian sciences as the development of a robust conceptual framework or grand, unifying theory that can serve as the template upon which we may inscribe our

contributions. Ten years later, Houser (2009) concedes that the development of a beach-dune model that transcends scale barriers and field site restrictions still eludes coastal scientists. While the stated goal of this research (defined below) is not to define such an ambitious model, there is current demand for more properly, accurately undertaken coastal meso-scale studies. The recent support for dynamic coastal restoration methods will provide the laboratory.

1.2. Thesis structure and research purpose and objectives

This thesis is structured around two results sections (2 and 3) derived from data collected between August of 2009 and 2010 at a beach-dune system located in the Wickaninnish Dunes, Pacific Rim National Park Reserve, British Columbia, Canada. These sections are bookended with an Introduction (Section 1) that sets the research context and Summary and Conclusions (Section 4) that reviews key findings of the research.

The general purpose of this research is to garner a better understanding of beach-dune evolution through developing novel methodology for detecting surface change that followed large-scale destabilization of the foredune. This purpose is explored through the following research objectives. Section 2 examines ten topographic survey datasets collected in a grid pattern over a beach, foredune, and transgressive dune complex (each area termed separate geomorphic units) by determining statistically significant changes between DEMs of each geomorphic unit, with significance evaluated using the student`s *t* distribution. Specifically, the objectives of this paper are to: i) identify multi-temporal and multi-spatial geomorphic changes between and over all geomorphic units at the study site, ii) refine a methodology for identifying said change, and iii) assess the effectiveness

of the implemented treatment (dynamic dune restoration) for increasing dune activity. This section has been submitted as a manuscript for peer review to the journal Earth Surface Processes and Landforms, and is currently in revision (March, 2012).

Section 3 utilizes tools provided by the field of spatial statistics, namely local Moran's I_i, to assess statistically significant patterns and change at the study site using the same dataset from Section 2. Specifically, the objectives of this paper are to: i) investigate the applicability of local Moran's I_i as applied to DEMs in a coastal setting, ii) quantify and describe geomorphic change following foredune destabilization, and iii) compare this method to a more conventional approach (Section 2). This section is a revised draft of a manuscript for submission for peer review to the journal Geomorphology.

2. Geomorphic and sediment volume responses of a coastal dune complex to invasive vegetation removal: Wickaninnish Dunes, Pacific Rim National Park Reserve, British Columbia, Canada

2.1. Abstract

Recently, there has been a shift from restoring coastal dunes as stabilized ecosystems to more dynamic systems that are geomorphically diverse, more resilient to erosion, and that offer greater ecosystem diversity, particularly for pioneering (and often endangered) species. This paper presents results from a large-scale dynamic restoration program implemented by Parks Canada Agency (PCA) to remove invasive marram grasses (*Ammophila* spp.) from a foredune-transgressive dune complex in Pacific Rim National Park, British Columbia, Canada. The program goal is to restore habitat for endangered Pink sandverbena (*Abronia umbellate var breviflora*) as required by the Canadian Species at Risk Act (SARA). Three sites were restored by PCA via mechanical removal of invasive marram grasses (*Ammophila spp.)* in September 2009. This study documents geomorphic and sediment mass exchange responses at one of these sites as derived from detailed DEM surveys of a 10 320 m^2 study area that spans three discrete geomorphic units (beach, foredune, and transgressive dune complex). Subsequent approximately bi-monthly total station surveys for the first year post-restoration are compared to a pre-restoration baseline LiDAR survey (August 2009) to quantify and describe morphodynamic responses and volumetric changes. Results show that the beach receives appreciable sediment supply via bar welding and berm development in the

winter (0.309 m^3m^{-2} between March and April) much of which is transported to the foredune and transgressive dune complex units in the spring (annual values of 0.128 and 0.066 m^3m^{-2}, respectively). This promotes rapid redevelopment of incipient dunes in the backshore, rebuilding of the seaward slope of the foredune following wave scarping, and localized extension of depositional lobes in the transgressive dune complex. The results of this study suggest that the foredune-transgressive dune complex at Wickaninnish Dunes has experienced enhanced aeolian activity and positive sediment volume changes over the first year following mechanical restoration.

2.2. Introduction

Coastal dunes are geomorphically significant features that store and cycle large amounts of sand. As such, they are key components of the coastal sediment budget (e.g., Short and Hesp, 1982; Hesp, 2002; Psuty, 2004) and they provide an important 'buffer' along shorelines subject to extreme and/or increasing storm surge and erosion impacts and more gradual sea-level rise (e.g., Davidson-Arnott, 2005; Houser et al., 2008; Mascarenhas and Jayakumar, 2008; Eamer and Walker, 2010). Sand dunes are also biological and ecologically significant (e.g., Grootjans et al., 2002; Hesp, 2002) as they provide critical habitat for many specialized endemic, migratory and endangered species (e.g., Wiedemann and Pickart, 1996) and as a natural resource and land use base (e.g., Nordstrom, 1990). In western Canada, less than 30% of the shoreline is partially sandy, with less than 10% of this consisting of dune-backed sandy beaches. Thus, there is recent interest in restoring coastal dunes from stabilized ecosystems with declining geomorphic (aeolian) activity to more dynamic ecosystems with increased aeolian activity and

improved habitat for early successional (and often endangered) species (Nordstrom, 2008).

Recent work on coastal dune restoration (e.g., van Boxel et al. 1997, Nordstrom 2008, Kollmann et al. 2011) suggests that a more dynamic landscape, wherein stimulation of natural geomorphic processes (e.g., aeolian activity) via vegetation removal, provides a more resilient ecosystem with more favourable ecological conditions for native and/or endangered species. This is a major shift from decades of restoration for coastal dune stabilization, which has been practiced for a range of purposes from forestry (e.g., Riksen et al., 2006) to wave erosion defense (e.g., Grootjans et al., 2002). Recent efforts to restore for more dynamic coastal dune landscapes provide distinct opportunities to quantify and examine sediment volume changes and transfer processes and resulting morphodynamic responses that, in turn, provide useful information for ecosystem management and coastal development (Nordstrom 2008).

Recent technological advancements have made for new developments in understanding and modelling the micro- to meso-scale morphodynamics of coastal dune systems, including: i) detailed airflow and sand transport experiments using high resolution ultrasonic anemometry and high-frequency electronic sand transport devices (e.g., Hesp et al., 2005; Walker et al., 2006; Lynch et al., 2008; Bauer et al., 2009; Davidson-Arnott et al., 2009; Walker et al., 2009a; 2009b; Jackson et al., 2011; Chapman et al., in review), ii) detailed mapping and quantification of beach-dune volumetric and morphological changes using Light Detection and Ranging (LiDAR) (e.g., Woolard, 2002; Sallenger et al., 2003; Houser and Hamilton, 2005; Saye et al., 2005; Eamer and Walker, 2010), iii) near-field remote sensing of sand transport events and morphological

responses (e.g., Darke et al., 2009; Delgado-Fernandez et al., 2009; Delgado-Fernandez and Davidson-Arnott, 2011), and iii) computational simulation modelling of dune dynamics (e.g., Baas, 2002; Baas and Sherman, 2006).

The dominant approach to analyzing beach-dune systems at the meso-scale is a sediment budget approach, where sediment eroded from one component of the system is accounted for by accretion in another component. Short and Hesp (1982), Psuty (1992), Sherman and Bauer (1993), Arens (1997), and Hesp (2001) have each made efforts to extend the approach to include various factors (e.g., nearshore inputs and morphology, fetch effects, aeolian contributions to foredunes) that refine the scope and/or role of inputs and outputs to the system. More recently, rapid, high resolution digital elevation models (DEM) generated from terrestrial and subaqueous LiDAR have emerged for characterizing volumetric and morphological responses, more in a mass-balance type approach, in beach-dune systems (e.g., Woolard and Colby, 2002; Sallenger et al., 2003; Houser and Hamilton, 2005; Saye et al., 2005; Eamer and Walker, 2010) and analytical methods using open-source software for accurate analysis of change detection are emerging (e.g., Wheaton et al., 2010).

The ability to use GIS and geostatistics to manipulate, visualize, and analyse spatial patterns in geomorphic data has become increasingly important in coastal research, especially at the meso-scale (Andrews et al., 2002). Various approaches have been used to quantify and examine coastal sediment mass balance and landscape responses using DEMs (e.g., Swales, 2002; Woolard and Colby, 2002, and Anthony et al., 2006). However, the mass balance approach requires careful consideration of how topographic and, thus, volumetric changes are defined and modelled so as to best

represent true changes within the system. Geostatistical interpolation methods (e.g., kriging) are often used to model the spatial continuity and trends in surface elevation data from a field of spatially discontinuous point measurements so as to produce a spatially representative DEM of a landscape at a given point in time. Spatial continuity models (e.g., variograms) associated with these methods are also useful for quantifying and potentially reducing errors associated with DEM generation from field data (Desmet, 1997). Spatial variograms have an experimental and model component. The experimental variogram provides the best estimate for spatial variation in a variable (i.e., difference in some z value over distance) and the parameters (e.g., sill, range, nugget, see Swales, 2002) are used to develop the best approximation model variogram. This model variogram has mathematically uniform properties, thus enabling it to be used in DEM generation (Swales, 2002).

2.2.1. Research Purpose and Objectives

The general purpose of this research is to accurately quantify and describe the sediment volume and resulting geomorphic responses within a recently destabilized foredune-transgressive dune system on the west coast of Vancouver Island, British Columbia, Canada. In particular, the study applies statistical change detection methods to high-resolution DEMs obtained from LiDAR and subsequent laser total station surveys to estimate seasonal sand volume changes and describe resulting geomorphic responses. As such, this research provides an initial assessment of the effects of mechanical vegetation removal to promote more dynamic habitat. Specific research objectives are as follows:

1. To quantify and describe significant seasonal volumetric and geomorphic changes within linked beach, foredune, and transgressive dune landscape units using detailed DEMs generated from recurrent site surveys for the first year following mechanical removal of vegetation.
2. To refine a methodology developed for fluvial settings for optimal sampling and processing of topographic survey data for accurate modelling and change detection within a coastal dune system.
3. To interpret initial landscape responses to dune destabilization and assess the effectiveness of the implemented treatment (complete vegetation removal) for enhancing dune morphodynamics.

2.3. Regional Setting

2.3.1. Study area and environmental setting

The study area is the Wickaninnish Dunes complex within Pacific Rim National Park Reserve (PRNPR), on Vancouver Island near Ucluelet, British Columbia, Canada (Fig. 1). This area hosts 1 to 5 m high vegetated foredunes that are prograding at a rate of approximately 0.2 m a^{-1} and are backed by the largest active transgressive dune complex on Vancouver Island (Heathfield and Walker, 2011). The 10-km long embayed beach has a mesotidal range (spring tide range ~4.2 m) and is exposed to energetic wave conditions (average winter significant wave height of 2.47 m and period 12.07 s). Beach-dune geomorphology varies slightly in Wickanninish Bay and the beach fronting the Wickaninnish Dunes has a shoreline length of approximately 4.2 km and an uninterrupted fetch to incoming winds and waves from the Pacific Ocean.

The climate in the study region is marine west coast cool (C_{fb}) per the Köppen classification with an annual average air temperature of 12.8°C (1971-2000) and high year-round precipitation (3305.9 mm). Rainfall occurs, on average, on 202.7 days of the year with 52% falling from October through January and only 18% falling during the summer months (May through August). Because of the mild temperatures and high precipitation, the dunes at this site support a number of native plant species, predominantly American dune (wildrye) grass (*Leymus mollis*), beach morning glory (*Convolvulus soldanella*), beach carrot (*Glehnia littoralis*), and yellow sand verbena (Abronia latifolia). Dominant species on the foredune, however, are the introduced American and European beach (marram) grasses (*Ammophila breviligulata* and *A. arenaria*, respectively). In the transgressive dunes, vegetation succession has lead to encroachment by native Kinnikinnick (*Arctostaphylos uva-ursi*) and Sitka spruce (*Picea sitchensis*).

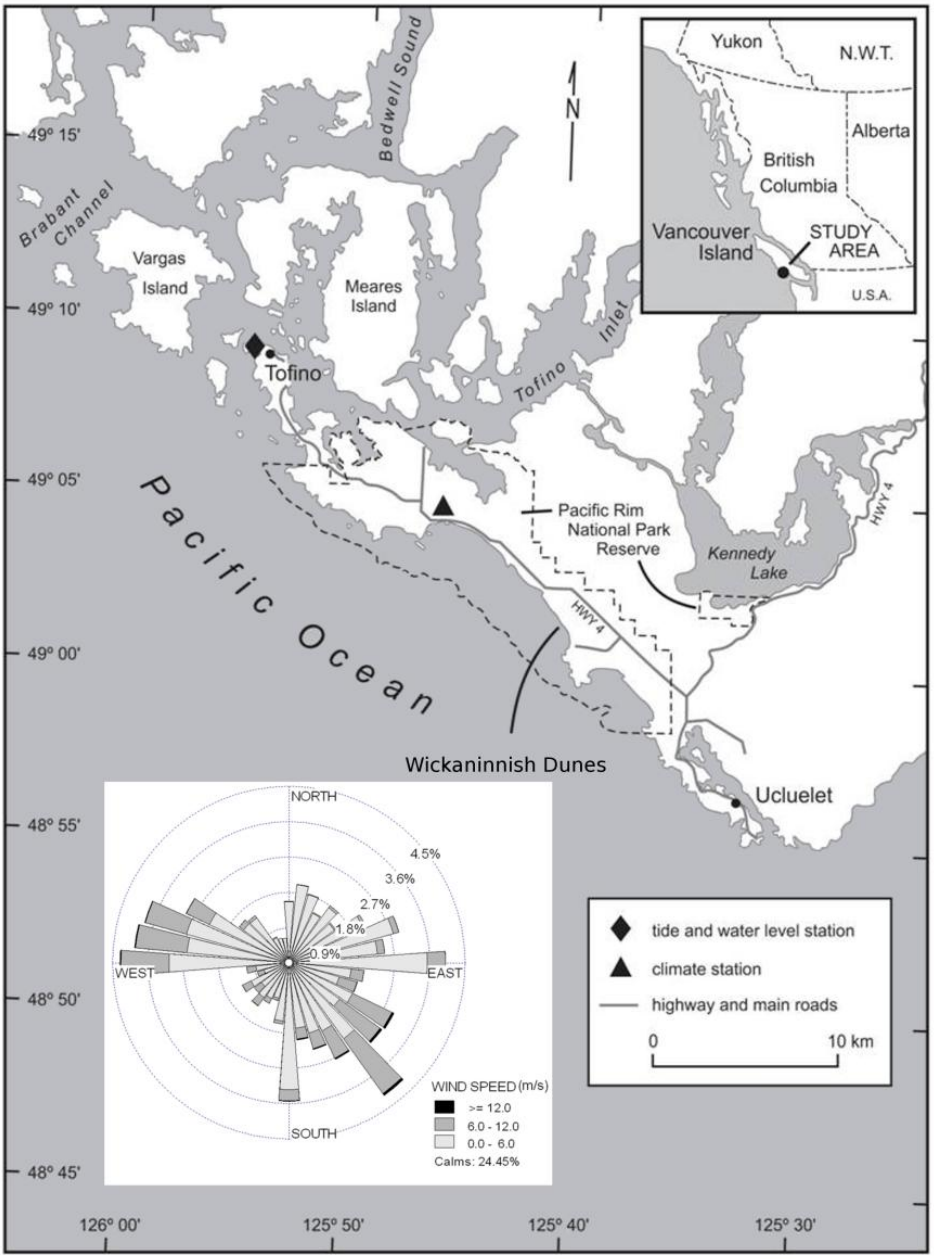

Figure 1. Study area showing the nearby town of Ucluelet and the climate station from which meteorological data were derived in Beaugrand (2010). Inset contains the annual wind rose for the study region. Data are from the Environment Canada climate station Tofino A [EC-ID 1038205] for the period 1971 to 1977 (from Beaugrand, 2010).

The introduced *Ammophila* is of special concern due to its aggressive expansion on foredunes, reduction of dune biodiversity, and ability to significantly alter foredune sediment budgets and morphodynamics (e.g., Wiedemann and Pickart, 1996; Hesp, 2002). At this site, *Ammophila* spp. have reduced habitat for the Grey beach pea vine

(*Lathyrus littoralis*), which is provincially red-listed as endangered, and the Pink sandverbena (*Abronia umbellate var breviflora*), which is federally red-listed as endangered under the Canadian Species at Risk Act (SARA). PRNPR is legally obligated under SARA to develop a recovery strategy for Pink sandverbena and a 5-year program of habitat restoration by Parks Canada Agency (PCA) is underway, which provides the opportunity for this research. It is hypothesized that dense *Ammophila* colonization of the foredune is responsible for reduced sand supply to, and resulting stabilization of, the transgressive dunes at Wickaninnish, which experienced a decline of 28% in active sand surface area from 1973 to 2007 (Heathfield and Walker, 2011).

The west coast of Vancouver Island experiences frequent WNW summer winds and strong SE winter storm winds (Eid et al., 1993; Beaugrand, 2010)(Fig. 1). The geomorphology of the transgressive dune complex (e.g., alignment of erosional blowouts and depositional lobes) suggests a dominant transport vector from the WNW driven by (drier) summer wind events, despite a resultant sand transport potential vector from the south (see Fig. 4, section 3.1). The combined effects of high precipitation during the winter months (which increase sand transport threshold during typical SE storm winds), local land and sea breezes, and topographic steering effects within the dunes and vegetation stands, alter local sand transport pathways that have maintained the north-westerly alignment of the transgressive dune complex.

2.3.2. Study site location and rationale

A stretch of approximately 3 km of foredune was identified by PCA in 2009 for mechanical removal of *Ammophila* to restore dynamic dune habitat. The first phase of

removal occurred on 21 September 2009 with approximately 200 metres of foredune cleared of vegetation on either side of four pre-existing, cross-shore coastal erosion monitoring profiles (Walker and Beaugrand 2008) (Fig. 2). Profiles extend from the beach over the foredune and transgressive dunes to the forest edge. At each site, invasive plant cover was removed mechanically by a backhoe equipped with a specialized finger bucket designed to reduce the amount of sand loss during the removal process.

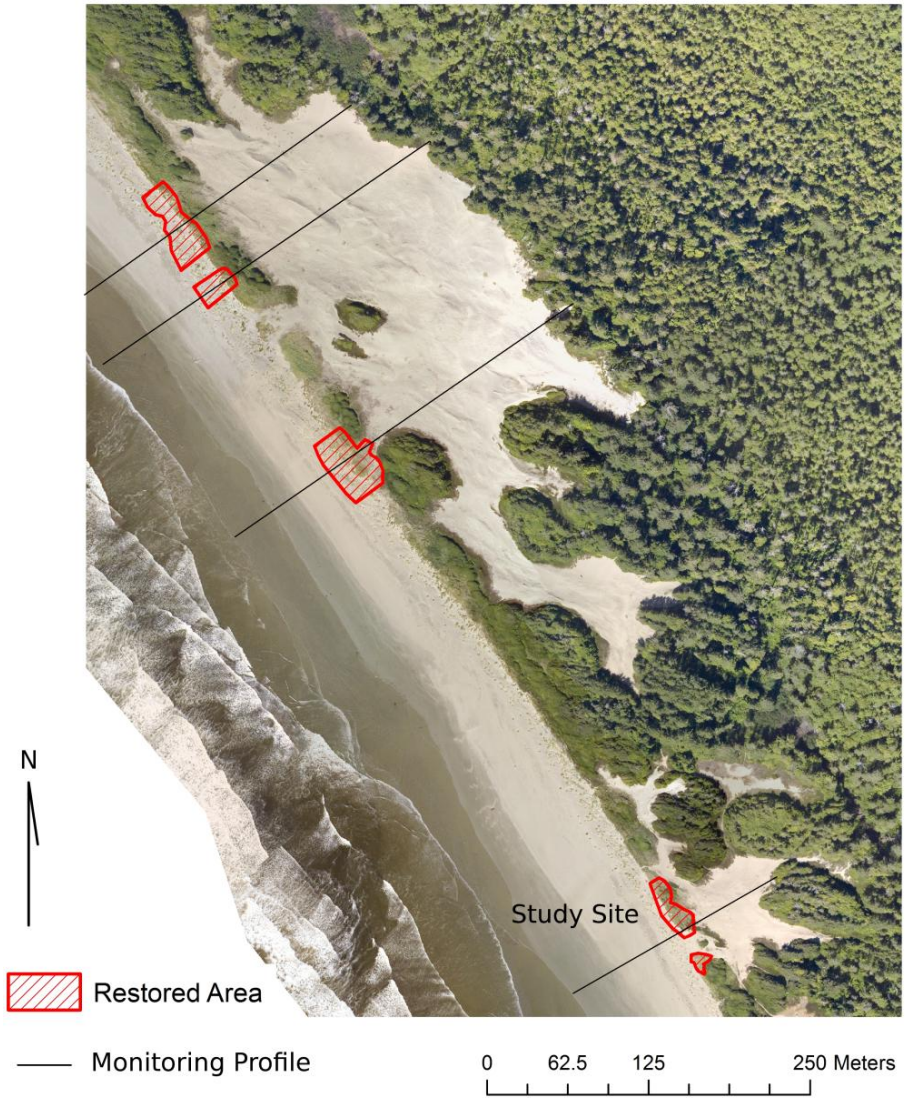

Figure 2. Map of study site with monitoring profiles from Walker and Beaugrand (2008), beach-dune complex under investigation, and foredune restoration coverage.

This study examines changes over the first year following vegetation removal at the southeastern-most site (Fig. 2), which is a smaller transgressive dune complex fronted by 75 m of fully denuded foredune and encompassed on all landward boundaries by forest vegetation. The study site had 10 320 m^2 of active sand surface and a perimeter of 924 metres, which remained essentially constant over the period of study. This site was selected as it provided a spatially discrete entity for quantifying and describing significant volumetric and morphological responses to the restoration treatment. The more northerly sites in the larger transgressive dune complex have considerably more active sand surface, much longer and open fetch distances, and, thus, appreciable lateral sand transfers and aeolian bedform migration between sites. Thus, it is more difficult to ascribe changes within these larger sites to the adjoined restoration treatment. However, the incomplete devegetation of the most northerly site in Figure 2, a similar beach and foredune morphology, and contemporaneous data collection at the site provided an ideal control site for volumetric responses of a site not fully restored. Darke et al. (in review) discuss the broader objectives and rationale for this restoration project and describe responses at other locations within the broader dune complex.

2.4. Methods

To assess changes in site geomorphology and sediment volume transfers, repeat (approximately bi-monthly) DEMs were produced using detailed topographic survey data imported into a multitemporal GIS database from which change detection maps and surface geostatistics were generated. The methodology for generating accurate DEMs

with quantifiable error using careful consideration of the geostatistical properties of the site is described below.

2.4.1. Data collection

An initial bare earth DEM base map of the entire Wickaninnish Dunes system was derived from airborne LiDAR flown on 27 August 2009 just prior to vegetation removal. Following this, laser total station surveys were conducted between August 2009 through August 2010 (Table 1) and were compared to the LiDAR reference dataset.

Table 1. Study site survey metadata including LiDAR base map and subsequent total station surveys. Bare sand surface area of the study site (10 320 m2) remained approximately constant during the period of study.

Date of Survey (Julian Day)	**Number of points**	**Point density (pt m^{-2})**	**Horizontal closing error**	**Vertical closing error**
27 August 2009 (LiDAR) (239)	11601	1.13	N/A	15 cm (assumed vertical accuracy)
24 September 2009 (267)	926	0.09	15.2 cm	0.20 cm
23 October 2009 (296)	455	0.04	8.0 cm	0.51 cm
8 December 2009 (342)	480	0.05	7.8 cm	1.11 cm
15 January 2010 (15)	501	0.05	8.2 cm	0.25 cm
5 March 2010 (64)	579	0.06	13.4 cm	0.60 cm
13 April 2010 (103)	532	0.05	2.2 cm	0.04 cm
30 May 2010 (150)	619	0.06	5.7 cm	0.47 cm
8 July 2010 (189)	781	0.08	15.0 cm	1.65 cm
14 August 2010 (226)	483	0.05	12.7 cm	1.56 cm

Topographic survey data were collected using a Topcon GTS226 laser total station. For every survey, the total station was re-sectioned (i.e., referenced) into a local grid of control points that were established using a Real Time Kinematic (RTK) GPS unit. As such, points were georeferenced on collection and required no post-processing. The survey data collection strategy was a systematic nested pattern (Chappell et al., 2003) (vs. a fixed positional grid of recurrently surveyed points) that captured detailed coverage of significant features and slope inflection points with grid densities of 0.04 to 0.09 points m^{-2} and vertical accuracies (closing errors) of 0.04 to 1.65 cm (Table 1) (Figure 3).

Beaugrand (2010) characterized the regional sand transport potential regime using wind data from the Environment Canada meteorological station Tofino A (EC-ID 1038205) located at Tofino Airport (Fig. 1) that only recorded 24-hour observations from 1971 to 1977. Unfortunately, a meteorological station installed at the Wickaninnish study site suffered instrument malfunctions during the first year of study and the dataset was not continuous enough to be useful. Per Arens (2004), and using the six years of Tofino Airport wind data, Beaugrand (2010) calculated annual and monthly sediment transport potentials (Fig. 4). These data are used to provide first-order estimates of sand transport potential conditions at the study site.

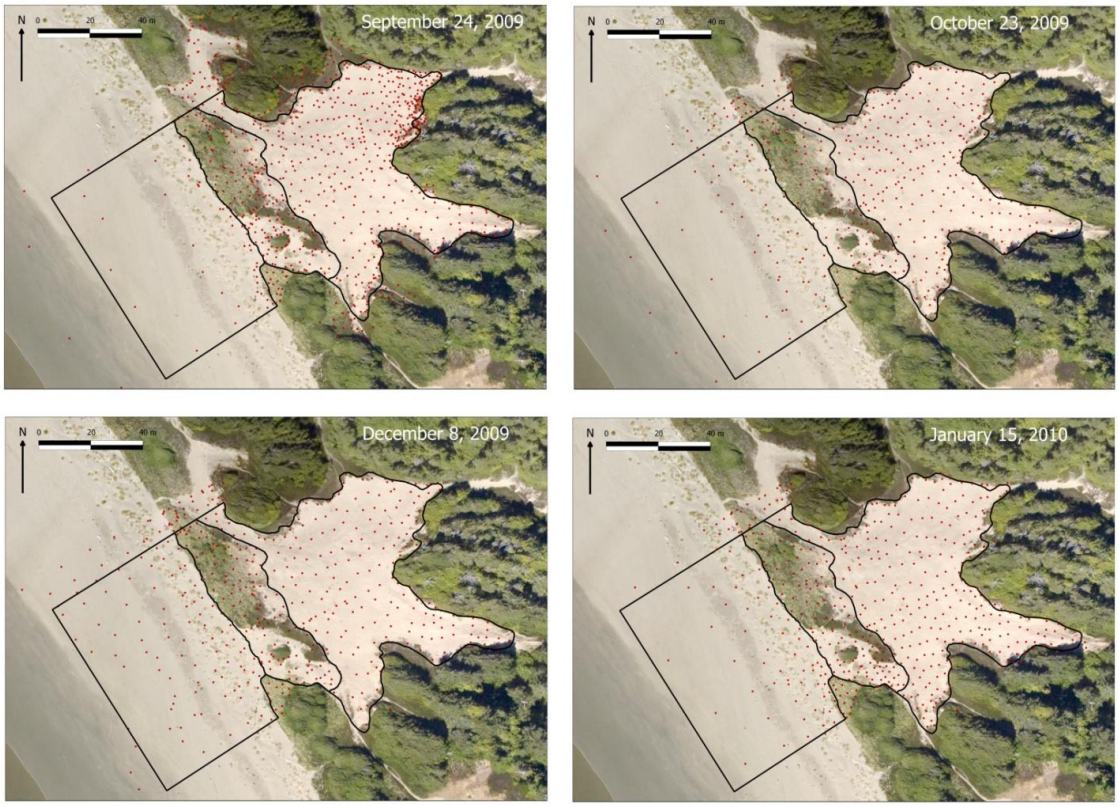

Figure 3. Survey points collected using the laser total station. Point patterns show the systematic nested technique, where surveyors follow a grid pattern, deviating to allow more coverage of areas with more topographic relief (continued on the following page).

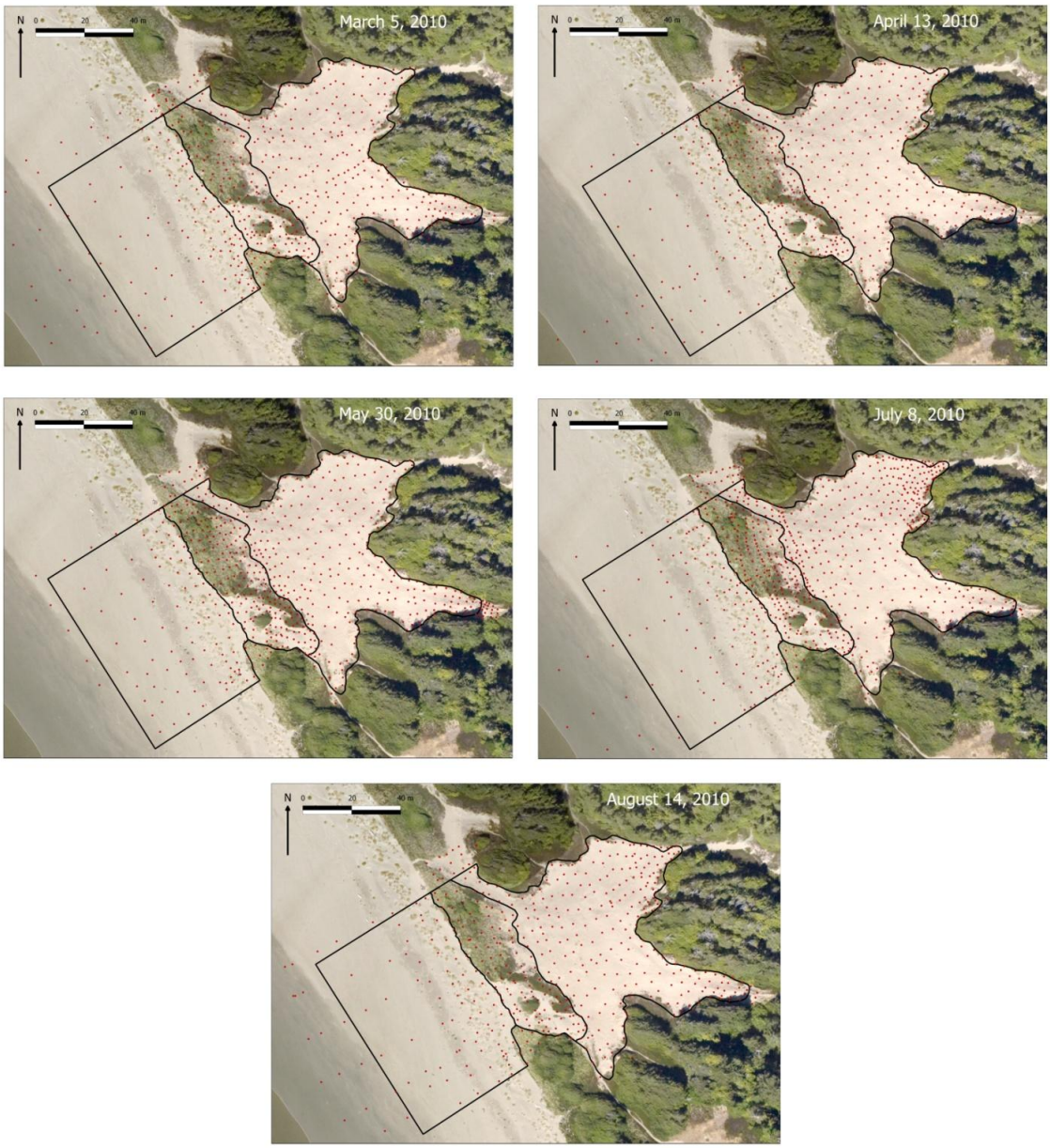

Figure 4. (cont'd) Survey points collected using the laser total station. Point patterns show the systematic nested technique, where surveyors follow a grid pattern, deviating to allow more coverage of areas with more topographic relief.

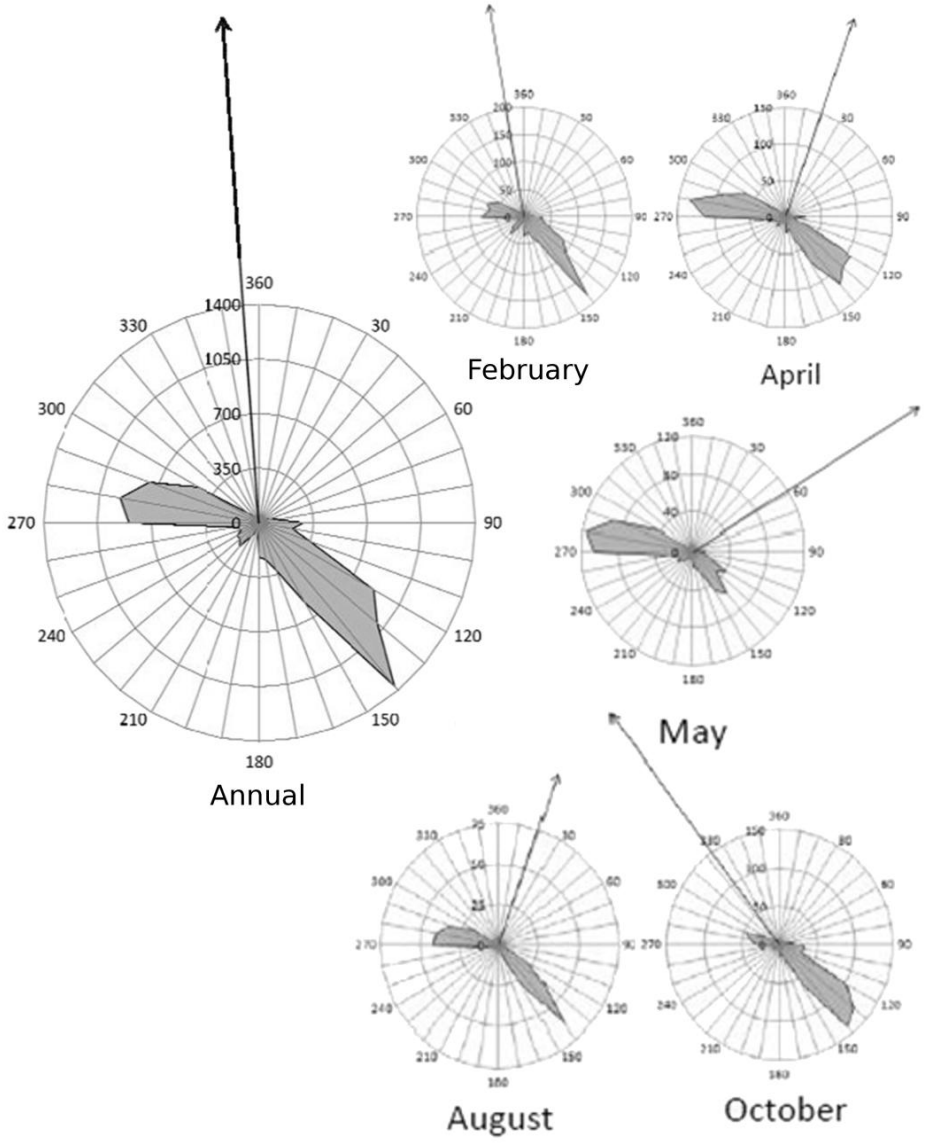

Figure 5. Transport potential and relative transport potentials for the study area (from Beaugrand, 2010) for specific months represented by DEM in Figure 6. Roses indicate the strongly bimodal annual transport regime (right) with transport from the WNW prevailing in summer and from the SE prevailing in winter (left). Axes represent azimuth (angle) and transport potential (magnitude) in $m^3m^{-1}month^{-1}$.

2.4.2. Data pre-processing

A digital orthophotograph mosaic was constructed for the study site using imagery obtained during the LiDAR mission. Interpretation of the photo mosaic, combined with field reconnaissance, was then used to delineate the study site into three discrete geomorphic units: beach, foredune, and transgressive dune complex (Fig. 5). This delineation made volumetric response comparisons within the same unit over time possible. Also, due to the different formative processes of features within the beach, foredune and transgressive dune units (i.e., swash zone dynamics, aeolian dominated transport, etc.), unit separation also allowed for more representative geostatistical modeling. This refines the interpolation method and provides some geomorphic rationale, as kriging takes directionality and variation distance, or orientation and size of features respectively, in to account. The beach unit was approximately 80 metres wide and was defined on the seaward margin by the limits of the survey and on the landward margin by the seaward extent of established foredune vegetation (e.g., *Ammophila spp.* and/or *Leymus mollis*). As such, the beach unit included an ephemeral incipient dune feature that formed within seasonal vegetation in the backshore (seen in Fig. 5). The foredune unit extended landward from this margin either to the landward extent of foredune vegetation or to the edge of depositional lobes extending from the foredune crest into the transgressive dune complex as identified in the original LiDAR survey. The transgressive dune complex was defined landward of this boundary and its remaining perimeter was defined by the extent of the active sand surface in the initial topographic survey. As above, the study site area (10 320 m^2) and outer boundaries (924 m) remained essentially constant over the period of study.

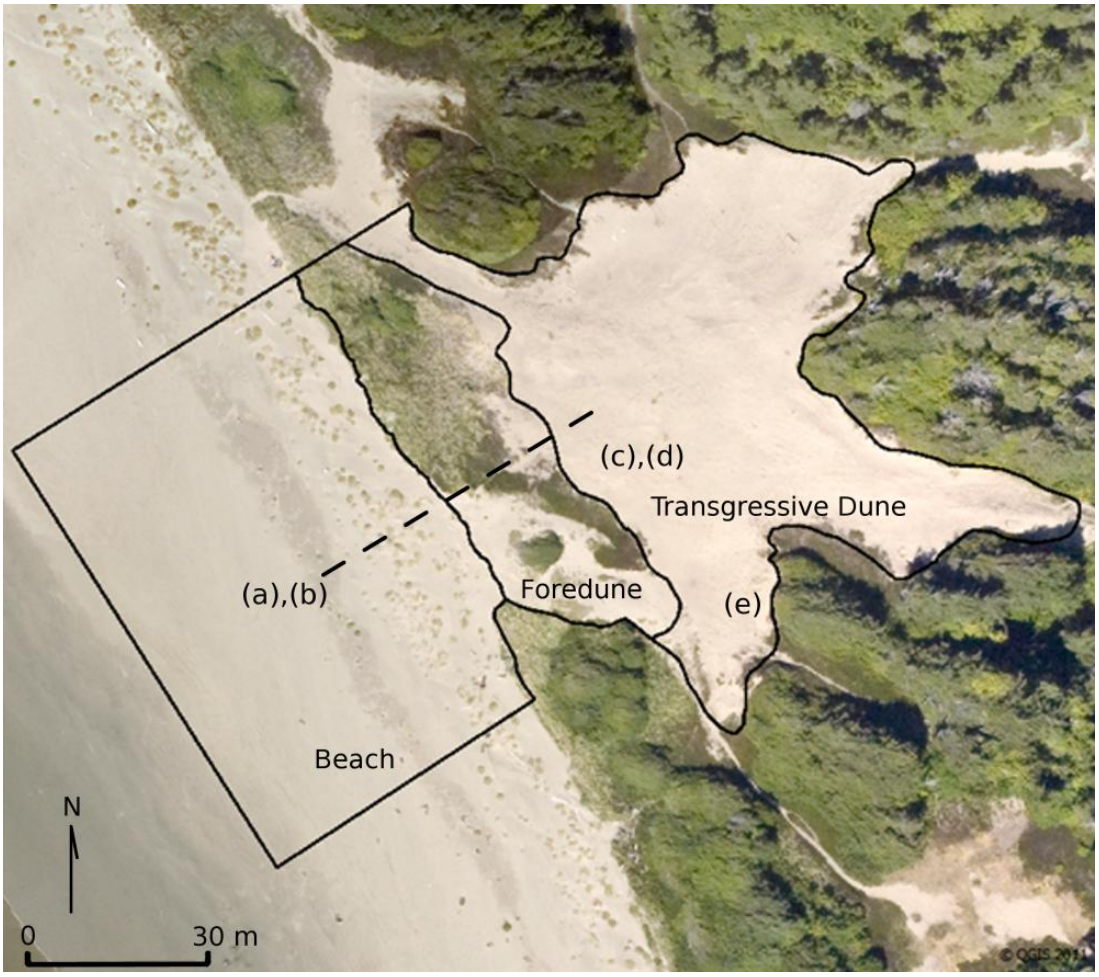

Figure 6. Map of the study area separated into discrete geomorphic units: beach, foredune and transgressive dune complex. The outer boundaries were defined by the outer limits of the survey with the smallest areal coverage. The inner boundaries (essentially bounding the shoreward and landward limits) of the foredune are defined in section 3.2. The dashed line gives the location of the extracted topographic profiles shown in Figure 6, chosen as a subset of the full profile (from landward boundary of the transgressive dune to lower beach) to highlight changes important to the restoration effort (the upper beach, foredune, and foredune lee). Bracketed letters show locations from which photos were taken for Figure 9 (a-e).

LiDAR and topographic survey DEM datasets were imported into QGIS© and shapefiles were generated. All datasets were then separated into geomorphic units using a spatial intersect join, which crops the point survey dataset using a polygon defined by the geomorphic unit area. These data were then exported to the R statistical software package and analyzed with two modules: i) the geostatistical package geoR (Ribeiro and Diggle, 2001) and, ii) RGDAL (R Geospatial Data Abstraction Library). geoR was used for the initial analyses of the spatial continuity of the surface elevation, variogram modeling, and to fill a DEM with gridded results (described below). RGDAL was used to export the DEM into a format in QGIS© (see section 3.4).

2.4.3. Geostatistical modeling

The spatial continuity of surface elevation was anisotropic (consistent with Swales (2002) and Chappell et al. (2003)), meaning there was distinct directionality in the variation of surface elevation. However, the experimental variograms generated were non-directional, which is recommended for studies with insufficient data to produce directional experimental variograms (Chappell et al, 2003). After the variograms were generated in geoR for each unit, initial researcher-driven best-fit model parameters were generated using an interactive tool allowing for model specification and manipulation. Gaussian or spherical models were found to best represent the semi-variance in every case (temporally across all three units). After initial parameters were generated and a model specified, model parameters were refined using ordinary least squares in geoR to determine a best fit for the model to the experimental variogram. geoR was also used to cross-validate the models fitted to the experimental variogram, which removes one datapoint from the set, predicts a surface model based on the remaining datapoints, and

computes the difference between the measured and exact point. This is repeated for each datapoint and accuracy statistics can be generated for the model.

Results of the cross-validation analysis (Table 2) indicated that the most accurate interpolation was within the transgressive dune unit (likely due to high point density allowing for more input to model specification), the most variance occurred within the beach unit (low point density), and the most consistency within the foredune (based on mean cross-validation and combined error). Combined uncertainty in each DEM was calculated as the sum of the 95% confidence interval surrounding the mean cross-validation error (based on mean and standard deviation of the cross validation results) plus the stated instrument precision (5 mm for the total station) (Table 2).

Table 2. Results of cross-validation for this study, showing mean cross-validation (c-v) error, standard deviation of the cross-validation error (c-v) across all sampled locations, and combined error (mean + 95% confidence interval + instrument precision).

Date of Survey (Julian Day)	Geomorphic Unit	Mean c-v error (m)	σ c-v (m)	Combined Error (m)
September 24 (267)	Transgressive Dune	-0.0025	0.21	0.0084
	Foredune	-0.0086	0.19	0.016
	Beach	-0.00071	1.00	0.057
October 23 (296)	Transgressive dune	-0.000092	0.25	0.0070
	Foredune	-0.016	0.28	0.028
	Beach	-0.026	0.27	0.041
December 8 (342)	Transgressive dune	0.0024	0.26	0.010
	Foredune	-0.0088	0.27	0.018
	Beach	-0.0014	0.18	0.011
January 15 (15)	Transgressive dune	-0.0018	0.22	0.0084
	Foredune	-0.0066	0.24	0.016
	Beach	-0.023	0.29	0.039
March 5 (64)	Transgressive dune	-0.00055	0.23	0.0073

	Foredune	-0.0067	0.28	0.016
	Beach	-0.0016	0.28	0.013
April 13 (103)	Transgressive dune	0.00070	0.33	0.0083
	Foredune	-0.0092	0.26	0.018
	Beach	-0.00074	0.24	0.012
May 30 (150)	Transgressive dune	0.00065	0.32	0.0080
	Foredune	-0.0093	0.19	0.016
	Beach	-0.00048	0.16	0.0080
July 8 (189)	Transgressive dune	0.00038	0.19	0.0064
	Foredune	-0.011	0.17	0.017
	Beach	-0.0042	0.16	0.012
August 14 (226)	Transgressive dune	0.0015	0.29	0.0088
	Foredune	-0.013	0.21	0.022
	Beach	-0.010	0.22	0.022
Average		-0.0058	0.27	0.017

2.4.4. DEM generation and cross-shore topographic profile extraction

An empty 1-metre grid was produced using tools in RGDAL for each geomorphic unit. Woolard and Colby (2002) suggest that a 1- to 2-metre resolution is sufficient to capture morphological and volumetric changes within most coastal dune systems. The data sampling strategy was designed to characterize geomorphic features within each unit with adequate point densities and, because the spacing of the LiDAR data was approximately 1 metre (Table 1), it is believed that this resolution was effective for characterizing significant landscape changes on a monthly timescale.

geoR was used to interpolate surface elevations for all grid cells based on each individual model (defined above) using an ordinary kriging algorithm at 4285, 1565, and 4470 grid cell locations in the transgressive dune, foredune, and beach units, respectively. Gridded results from the kriging algorithm were then exported in ESRI ASCII (.asc)

format using RGDAL as geoR does not produce files usable outside of R. These grids were then imported into QGIS© for cropping into unit polygons and further analysis.

To complement the three-dimensional volumetric estimates and surface mapping from the DEMs, and to provide additional visualization of two-dimensional changes across the units, cross-shore profiles were extracted from the interpolated DEMs along the transect coordinates of the existing coastal erosion monitoring profiles (Walker and Beaugrand, 2008). A detailed subset of these profiles showing the upper beach and foredune (located in Fig. 5) are presented in Figure 5 and discussed in section 4.1.

2.2.5. Volumetric calculations and geomorphic change map generation

DEMs were imported to the Geomorphic Change Detection (GCD) software package (Wheaton et al. 2010), which was developed primarily for morphological sediment budgeting and change detection in river systems. The software calculates volumetric changes in sediment storage from repeat topographic surveys, quantifies associated errors, and identifies statistically significant changes. An important part of the functionality of the GCD software is the ability to account for type 1 error, where a true null hypothesis (no surface change) would be incorrectly rejected, by removing survey and interpolation noise from the results. The combined error (described in 3.3) was entered into the GCD software wherein significant changes were calculated based on the student's *t* distribution and a test statistic (Wheaton et al. 2010):

$$t = \frac{|zDEM_{new} - zDEM_{old}|}{\sigma DoD} \quad (1)$$

where $zDEM_{new}$ and $zDEM_{old}$ are the interpolated elevations in a specific grid cell of subsequent surveys and σ_{DoD} is the characteristic error in this case represented by propagated errors:

$$\sigma_{DoD} = \sqrt{(\epsilon_{new})^2 + (\epsilon_{old}} \quad (2)$$

where ε_{new} and ε_{old} are the individual survey errors (combined errors from Table 2). Significant volumetric change estimates for each DEM were calculated in GCD by essentially subtracting grid cell elevations of the baseline LiDAR DEM from the survey DEM (Table 3). Difference maps for all units and survey dates were also produced and imported into QGIS© for overlay onto site orthophotographs and graphical preparations (Fig. 7). This provides a sequence of maps indicating the progression of statistically significant surface changes within the beach-dune system since restoration.

2.5. Results

2.5.1. Cross shore topographic profile changes

For the extracted cross-shore profiles (Fig. 6) and volumetric change detection maps (Fig. 7), only five of the nine interval datasets were chosen (23 Oct, 5 Mar, 13 Apr, 30 May 30, 14 Aug) for clarity and ease of interpretation of distinct changes within the landscape relative to the pre-restoration (LiDAR) survey of 27 August 2009.

The cross-shore profiles show two-dimensional changes in beach-dune topography relative to the pre-restoration survey. In general, the beach portion of the profile exhibited a general accretion response from the upper intertidal to the incipient dune region in the backshore by as much as 0.5 metres over the year following the

baseline LiDAR survey. The incipient dune zone seaward of the foredune toe also experienced marked accretion between the initial survey and October, then both areas eroded over the winter via high wave runup events that removed the incipient dune and caused scarping and retreat of the lower seaward (stoss) slope by ~2 m between October and March surveys. The incipient dune rebuilt rapidly by ~0.3 m (3.5 mm day^{-1}) by vertical accretion of aeolian sands in the spring (March to May) and a foredune ramp developed to infill the eroded scarp at the toe of the foredune (Figs. 9a and b). The toe and incipient dune zone regions remained relatively stable through the summer.

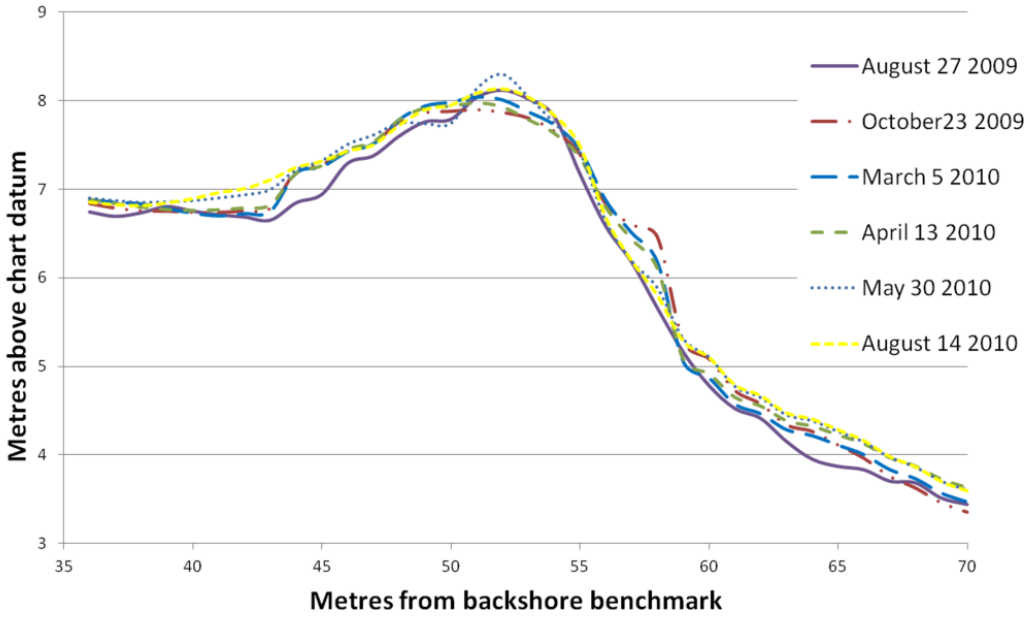

Figure 7. Topographic cross-shore profiles extracted from interpolated DEM data. Survey dates selected are those used in the geomorphic change maps in Figure 7.

On the established foredune, comparison of the pre-restoration profile to those from subsequent surveys shows that most of the stoss slope had aggraded, except in the crest region. Here, erosion of ~0.3 m occurred between the pre-restoration profile to the October survey, which likely reflects sediment removal during the mechanical restoration

process, then the crest built quickly by ~0.5 m (2.3 mm day^{-1}) to the May survey, followed by erosion of ~0.2 m (2.6 mm day^{-1}) by August. The distinct ridge feature formed on the lower stoss slope of the foredune (most extensive in the October survey, Fig. 6) was also likely a product of the vegetation removal process in September and this ridge essentially disappeared between March and May. Thus, as a result of equipment activity and vegetation removal, the foredune had a slightly lower, wider profile compared to the pre-restoration LiDAR survey in August 2009. Over time, however, it appears that the surplus sediment on the seaward slope was moved landward via aeolian transport to rebuild and steepen the crest. Generally, the mid-stoss slope appears to be a location of sediment bypassing and minimal morphological change between October and August surveys. By August, nearly one year following the mechanical restoration activity, the seaward profile of the foredune attained a very similar form, with slight progradation on the lower stoss and toe (~1 m) perhaps resulting from enhanced supply of sediment to the beach.

Leeward of the crest there was much activity and general accretion of sediment on the lee slope by as much as 0.4 m over the year following the restoration removal. In the immediate lee of the crest, slight deposition (~0.2 m) occurred between the pre-restoration and March surveys followed by notable erosion between March and May (~0.3 m or 3.5 mm day^{-1}) then deposition again to counter most of this erosion between May and August surveys via sediment eroded from the crest region. Further landward, a new depositional lobe (~5 m long and approximately 0.4 m deep) developed and extended leeward rapidly between April and August surveys.

2.5.2. Geomorphic and sediment volumetric change responses

Figure 7 shows select surface change detection maps that visualize statistically significant, seasonal responses of the beach-dune system following vegetation removal at select dates. Corresponding volumetric change values for these intervals, and those intervening, are provided in Table 3. Over the entire year, all three geomorphic units experienced a net increase in sediment volume with the beach receiving +834 m^3, the foredune +200 m^3, and the transgressive dune +284 m^3. Normalizing these values by the surface area of each unit (e.g., m^3 m^{-2}) provides an effective depth of sediment accretion (+) or erosion (-). Overall, the beach saw an average accretion of +0.187 m, the foredune +0.128 m, and the transgressive dune +0.066 m.

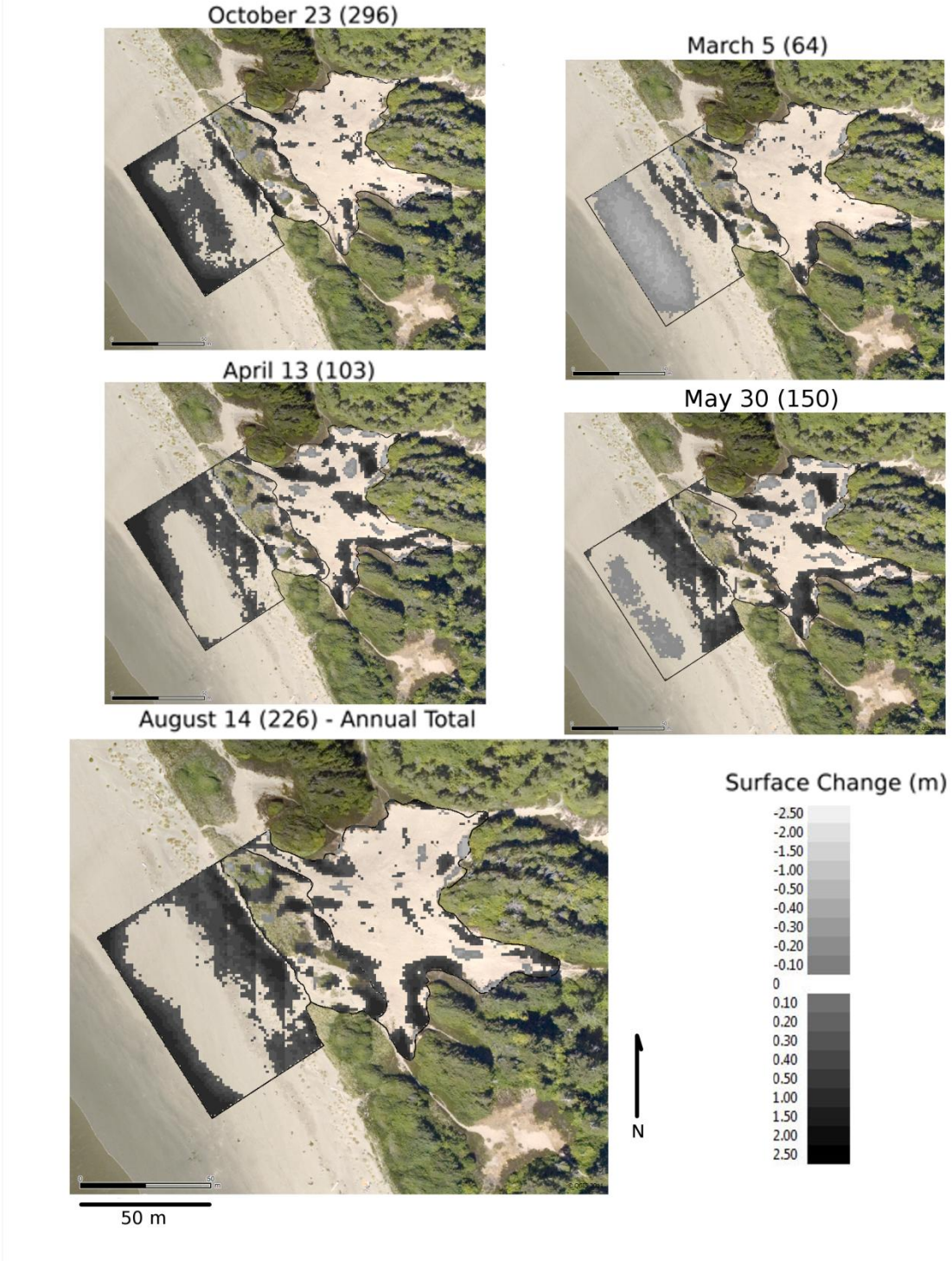

Figure 8. Geomorphic change maps of the study area selected to show beach and dune trends. Survey date and Julian day in brackets are shown above each map.

Table 3. Estimates of statistically significant sediment volume changes determined using the GCD methodology (Wheaton et al. 2010). Area-normalized values (m3 m-2) provide an effective depth of average sediment accretion (+) or erosion (-) within each unit.

	Volumetric change from LiDAR baseline (m^3) and area-normalized (m^3 m^{-2})		
Survey (Julian Day)	**Beach: 4470 m^2**	**Foredune: 1565 m^2**	**Transgressive dune: 4285 m^2**
September 24 (267)	+715 (+0.160)	+18 (+0.012)	+201 (+0.0469)
October 23 (296)	+977 (+0.219)	+101 (+0.0645)	+123 (+0.0287)
December 8 (342)	+373 (+0.0834)	+137 (+0.0875)	+179 (+0.0417)
January 15 (15)	-101 (-0.0226)	+91 (+0.058)	+126 (+0.0294)
March 5 (64)	-679 (-0.152)	+113 (+0.0722)	+118 (+0.0275)
April 13 (103)	+721 (+0.161)	+97 (+0.062)	+345 (+0.0805)
May 30 (150)	+410 (+0.0917)	+129 (+0.0824)	+373 (+0.0870)
July 8 (189)	+917 (+0.205)	+142 (+0.0907)	+204 (+0.0476)
August 14 (226) (Annual total)	+834 (+0.187)	+200 (+0.128)	+284 (+0.0663)

Annually, most of the accretion on the beach occurred within the incipient dune zone and the upper beach, although much of this sediment is eroded often by winter storms (Heathfield and Walker, 2011), as evident in the seasonal results presented below and consistent with the results from the extracted profiles. Within the foredune, accretion occurred within depositional lobes that extend leeward from the crest. In the transgressive dune complex, accretion occurred mostly via extension of depositional lobes on both from the lee side of the foredune into the transgressive dune complex and on the far east (transgressing) side of the site.

The beach surface exhibits the highest total volumetric change (1596 m^3 between the maximum and minimum relative to pre-restoration) and is the only geomorphic unit to experience erosion relative to the intial LiDAR survey prior to disturbance. Net erosion within the beach unit was captured by the January and March surveys (Table 4) during higher energy wave conditions in the winter months, as expected. Sediment

accretion occurred rapidly between March and April (1400 m^3 or 36 m^3 per day), however, with the onset of more transporting wind events (Figure 4) and lower energy long-period swell conducive to onshore movement of sediment in the nearshore. Migration of a rip cell megacusp embayment before the May survey was associated with a decline in the accretion volume and a steepening of the beach below the incipient dune zone. Seasonal vegetation growth in the incipient dune zone and upper beach then favoured the deposition of sediment in spring and summer months (April through August) as evident in the topographic profiles (Fig. 6).

Accretion within the foredune following vegetation removal in early September was low (18 m^3) but increased by an order magnitude by December (137 m^3). As noted in the cross-shore profiles, the stoss slope of the foredune unit experienced notable scarping in response to increased winter wave activity and high water events from December through March. By late spring and summer, accretion resumed largely in the form of large depositional lobes on the southeastern end of the foredune unit, perhaps reflective of increased sand transport potential from the NW (Fig. 4) and drier conditions during this time (200 m^3 by August).

Initial responses within the transgressive dune complex showed sporadic net accretion by September and little net change in the winter months (-83 m^3 September to March). By spring (April), accretion in the transgressive dune complex (227 m^3) occurred mostly by migration of discrete dune features that eventually fed into the precipitation ridge on the eastern edge of the dune by August. Additional accretion in this unit occurred on the border with the foredune unit, where depositional lobes migrated into the transgressive dune.

2.6. Discussion

2.6.1. Methodological implications

The methodology employed in this study builds on previous research using DEMs to identify and quantify geomorphic and volumetric change in sedimentary landscapes. It is often difficult, however, to compare results from such studies largely due to inconsistencies in DEM generation and different handling of error (e.g., Andrews et al., 2002; Swales, 2002; Mitasova et al., 2005; Anthony et al., 2006; 2007; Wheaton et al., 2010). This study provides an easily implemented, cost effective, and precise methodology that uses common surveying technologies and open-source software to provide an accurate and repeatable method for identifying significant geomorphic and sediment volume changes in dune landscapes. This study utilizes the distinct geostatistical signatures found within discrete landscape units that often have directionality in their morphology and/or sand transport pathways. Coupled with proper application of the kriging interpolation method, this produces more accurate and systematically repeatable DEMs from floating point cloud data, typical of field surveys.

The methods for error quantification developed by Wheaton et al. (2010) were useful for providing a more systematic consideration of uncertainty via incorporating measurable quantities of both instrument and interpolation error using a statistical test. Wheaton et al. (2010) state, however, that lower point densities may result in greater areas within the DEM used for change detection analysis yielding insignificant results. This approach (Wheaton et al., 2010) is useful in rapidly and sometimes, subtly, changing coastal beach-dune systems as it provides a repeatable and systematic method for distinguishing between simply small, yet observable changes in repeat surfaces and those

that are truly statistically significant, thereby avoiding the use of arbitrary thresholds. Further integration and refinement of this methodology into geomorphic applications where lower point densities are common or logistically defined, or application to higher resolution aerial or ground-based LiDAR surveys, is recommended.

Separation of the Wickaninnish Dune complex into distinct geomorphic units allowed for increased accuracy in surface modeling and provides a straightforward and logical method for the analysis and interpretation of sediment exchanges and related geomorphic responses. While comparison of cross-validation results with interpolations of the entire study site revealed that the methodology shows small increases in interpolation accuracy, utilization of variogram directionality (per Swales, 2002) may yield different results. Also, the generation of separate difference surface maps for each unit in the GCD software allows the researcher to create custom accuracy bounds on each unit to generate DEM-specific volumetric uncertainties, useful in creation of separate GCD maps.

2.6.2. Volumetric and geomorphic responses of the beach-dune system to vegetation removal

Figure 7 summarizes observed volumetric changes (Table 3) within geomorphic units of the beach-dune system for one year following the mechanical removal of vegetation from the foredune. The beach shows significant accretion in the fall and early winter (September to October) totaling 977 m^3 (or 0.219 $m^3 m^{-2}$) resulting from bar welding and berm development during this time, followed by beach steepening and erosion during winter months (-1656 m^3 or -0.370 $m^3 m^{-2}$ from October through March)

when wave energy and the frequency of high runup events is higher. In spring and summer months (March through August), the beach maintains a positive sediment volumetric change (1513 m^3 or 0.338 $m^3 m^{-2}$) that is very similar to that in the fall months (relative to the original state) and results from lower energy swell waves and low amplitude bar welding to the beach. Overall, the beach unit maintains a positive sediment volumetric change of 834 m^3 (0.187 $m^3 m^{-2}$) over the year following the restoration activity. This influx of sediment is essentially independent of the restoration effort on the foredune and provides an appreciable supply of sediment for potential landward delivery to the dune systems. Without longer-term observations, however, it is uncertain as to how representative this positive annual volumetric change is for Wickaninnish Beach. Heathfield and Walker (2011) documented positive rates of shoreline progradation at Wickaninnish Beach (0.2 m a^{-1}) and the adjoined Combers Beach (1.1 m a^{-1}) from analysis of historical aerial photographs, which suggests that these beaches maintain a net positive onshore sediment volumetric change.

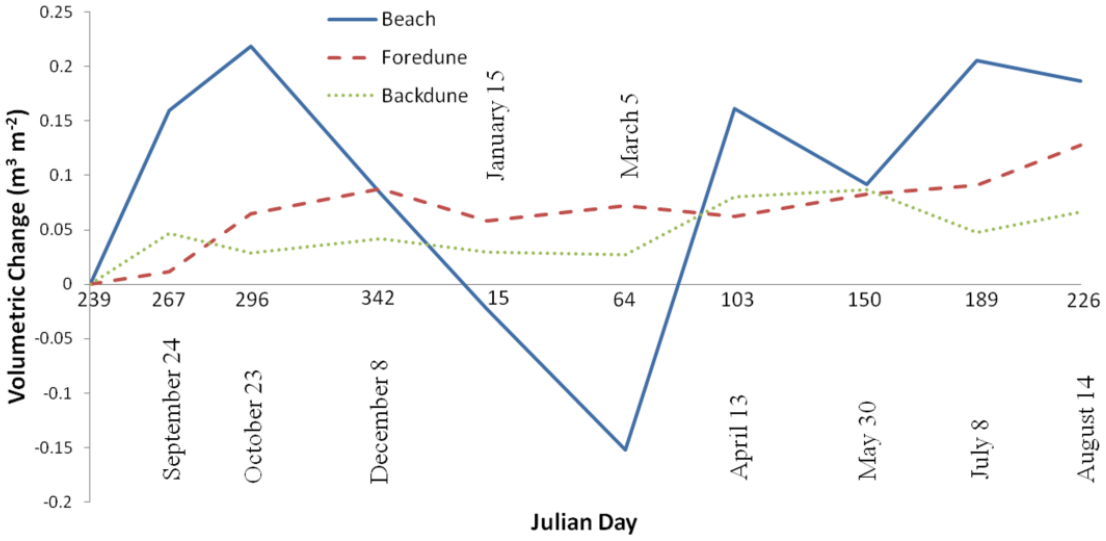

Figure 9. Area-normalized volumetric results determined to be statistically significant based on GCD methodology described above.

The foredune experiences slight initial accretion (18 m^3 or 0.012 $m^3\,m^{-2}$) after the vegetation removal in September followed by an order of magnitude increase in deposition by October (83 m^3 or 0.0633 $m^3\,m^{-2}$). Although the foredune unit experienced a net positive sediment volume change, erosion of ~2 m of the seaward slope occurred between October and March by high wave runup that also eroded the incipient dune. Despite high average aeolian sand transport potential during these months (Table 2), rebuilding of the foredune scarp and incipient dune does not occur perhaps because average resultant transport potential vectors are predominantly along- to offshore oriented (Fig. 4) and/or wet seasonal climate conditions limit aeolian activity. In the spring and early summer, however, the foredune sees increased accretion overall as the upper beach receives increasing sediment supply. A sand ramp also develops rapidly (5.0 mm day^{-1} of accretion between April and May) to infill the eroded scarp at the foredune toe (Figs. 9a, b) and remaining sediment from the secondary ridge on the lower stoss slope of the

foredune (a remnant of the restoration activity) is transported landward for vertical growth at the crest and landward extension of a depositional lobe in the lee (Figs. 6, 7). Overall, in the year following the restoration activity, the foredune shows a positive sediment volume change of 200 m^3 (0.128 $m^3 m^{-2}$), which is about 24% of that of the adjoining beach, and the dune profile returns to a form similar to the pre-restoration profile with some progradation in the toe region and enhanced deposition in the lee (Figs. 6, 7, 9c, d).

Figure 10. (a,b) Vantage photos of the foredune from March and July. Note the scarping and rebuilding of the foredune ramp, and accretion in the incipient dune zone in the upper beach with associated seasonal vegetation. (c,d) Vantage photos of the lee-side of the foredune for December and April. Deposition lobe is developing, killing off of perennial vegetation, and liberating dune sediment in the area for transport further into the transgressive dune. (e) Transgression on the eastern edge of the transgressive dune complex. See Figure 5 for photo locations.

The transgressive dune complex is perhaps the only unit within which geomorphic and sediment volume responses are controlled entirely by aeolian activity. Sediment influx to the transgressive dune complex is high immediately following the restoration activity in September (201 m^3 or 0.047 $m^3 m^{-2}$) and an order of magnitude greater than that on the foredune. This may reflect landward transport of sediment from the disturbed foredune during this time, as evident in the cross-shore profiles (Fig.5). From October through March, the transgressive dune complex continues to show accretion trends and absolute volumes similar to the foredune, although distributed over a larger surface area (Table 4). Accretion volume within the transgressive dune complex increases rapidly (5.675 m^3 day^{-1}) between March and April while slower deflation of the foredune (-0.4 m^3 day^{-1}) occurs during the same time period. Sand accretion in the transgressive dune complex continues to increase through May and it is speculated that this may reflect both high average resultant transport potential that is oriented more onshore in early summer (Fig. 4) as well as improved sand transport pathways following sand ramp development and infilling of eroded scarps on the seaward slope (sf. Christiansen and Davidson-Arnott 2004; Davidson-Arnott et al. 2005). As with the foredune, the transgressive dune also receives additional sediment mass (+284 m^3 or 0.066 $m^3 m^{-2}$) in the year following the restoration activity while its area of active sand surface remains essentially constant (4285 m^2).

2.6.3. Ascribing observed responses to the impacts of dune restoration

To fully assess the impacts of a dune restoration treatment (in this case, mechanical removal of invasive vegetation) on landscape sediment volume change and geomorphic responses, contemporaneous control data are required. Ideally, this would involve concurrent surveys within a co-located site of identical geomorphology wherein vegetation has not been removed. Such situations often do not exist, however, for various logistical reasons (e.g., lack of suitable control sites, fieldwork costs) and program mandates (i.e., restoration agency objectives and timelines that do not match or consider research objectives and timelines). In this study, conventional contemporaneous control data did not exist given the size, extent and geomorphology of the site as well as the rapid timing and broad implementation of the PCA vegetation removal campaign. However, the pre-restoration LiDAR-derived DEM provides a baseline reference dataset against which subsequent landscape changes are normalized. Also, two comparable sets of data are available that provide an account of both what trends existed prior to restoration at the study site, and what geomorphic response was observed at a site of similar geomorphology during the study period.

Cross-shore profiles measured one year prior to restoration and one year following, modified from Darke et al., (in revision) (Fig. 10), are provided to illustrate foredune morphology change both prior to and following the restoration treatment. These profiles were measured at the same location as the extracted profiles shown in Figs. 5 and 6. Changes between 2008 and 2009 (representing one year of change prior to restoration) indicate deflation in the lee side of the foredune of -0.2 m. Conversely, between 2009 and 2010 (representing one year following restoration), there is accretion of +0.5 m in the foredune lee. These results, obtained by a different methodology,

correspond well with the results from section 4.1, where accretion of +0.4 m in the lee of the foredune was documented. Thus, Figure 11 indicates that increased sediment inputs past the upper beach and the development of depositional lobes in the lee side of the foredune did not occur at least in the year prior to restoration. This suggests that one of the stated goals of this restoration, to increase landward sediment transfers, has been achieved over this two year period.

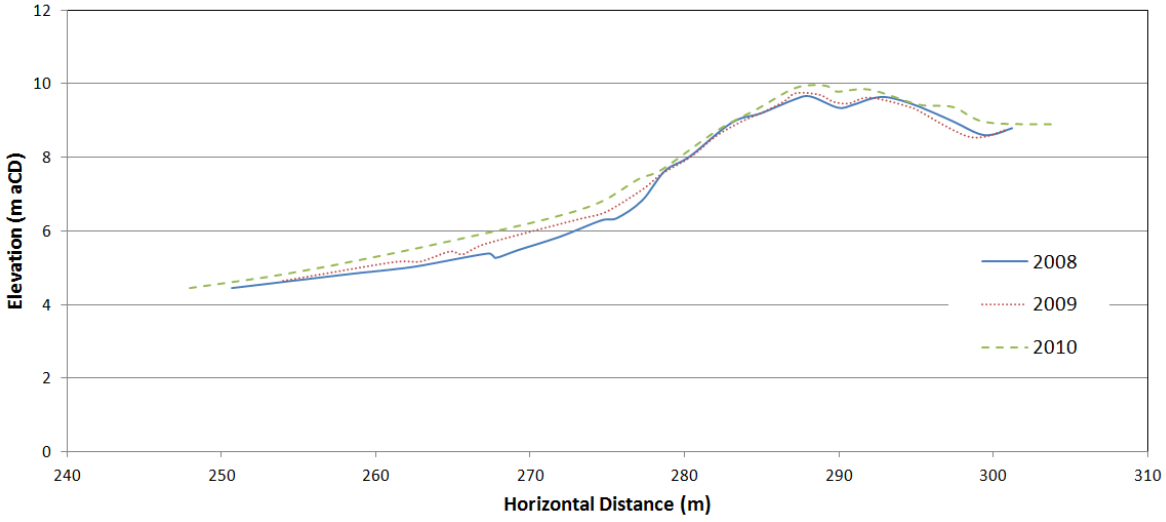

Figure 11. Topographic profiles modified from Darke and Walker (2010) for the study site, showing a year of change prior to and a year following restoration. Note that issues with the chart datum definition don't allow for direct overlay on Fig. 6, however form and relative change agree with data gathered for this study.

In addition to the cross-shore profile comparison, a surface change DEM for the same year of observation was generated (Fig. 11 as modified from Darke et al., in review) for a site ~600m to the northwest of the study site (northern-most 'restored area' polygon in Fig. 2). In relation to conditions at the study site, beach fetch (both ~100m from the WNW at mean low tide) and foredune morphology (both ~ 4m high, near-equivalent stoss slopes) are comparable. However, vegetation removal on the foredune further north

was not extensive (i.e., only the lower 5 m was devegetated, see Figure 11) and did not permit sand transfer via saltation between the beach and the transgressive dune complex. Darke et al., (in review) provide more in-depth analyses of this site, however, for the purposes of this paper, this location provides some contemporaneous control of volumetric beach-dune responses where vegetation was not fully removed. Beach trends are similar, with accretion reaching depths of 1.5m in the upper beach at both sites. Accretion in the foredune is limited to a 10m stretch at the landward extent of the restoration area, which is likely fed by sediment from erosion at the foredune toe and deposited when encountering the increased surface roughness provided by remaining vegetation. There is no significant deposition observed in the lee side of the foredune crest at this site (i.e., along the landward margin of the foredune unit). This is not the case at the study site (Fig. 7), where a large amount of foredune accretion was located. Area normalized sediment volume change also indicates nearly a 50% increase in foredune accretion at the study site (+0.128 m^3 m^{-2}) versus at the control site (+0.086 m^3 m^{-2}). Thus over the same period of study, a control site of comparable geomorphology with vegetation only removed from the foredune stoss saw little additional sediment inputs in, and over, the foredune. Enhanced aeolian activity and increased sediment exchanges over the foredune are therefore attributed to complete devegetation of the foredune at the study site.

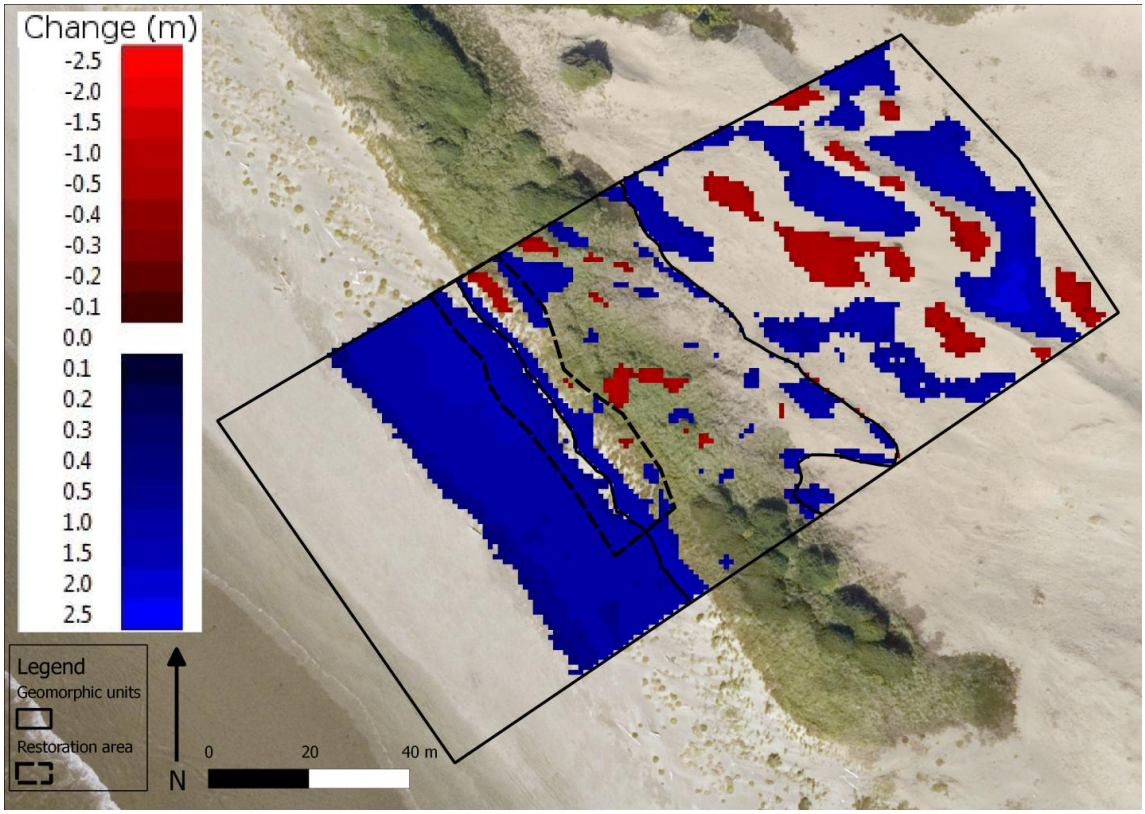

Figure 12. Annual geomorphic change map of an area roughly 600m to the NW from the study site, modified from Darke et al. (in review). Dashed line represents the extent of vegetation removal undertaken in September, 2009 (note the landward extent). Solid line represents geomorphic unit delineations (as in Figure 5). Note the absence of large, developed depositional lobes in the lee of the foredune (i.e., up against the landward extent of the foredune unit). This image is provided for comparison to the "Annual total" geomorphic change map from Figure 7.

2.6.4. Effectiveness of mechanical restoration for enhancing foredune morphodynamics

Essentially, dynamic dune systems are those within which natural aeolian processes take place and/or are enhanced (Nordstrom, 2008). The restoration strategy employed by PCA at the study site is essentially a 'process management' approach (e.g., Riksen et al., 2006) that removes vegetation over large areas with no specific pattern (i.e., broad scale removal on the foredune) and distinct, artificial borders in an effort to

enhance aeolian activity and dune morphodynamics. In stabilized dune systems, aeolian processes are relatively inactive or absent and the landscape is often colonized by perennial grasses and woody shrub and tree species with a high density, whereas dynamic dune systems often have lower vegetation densities and the vegetation present is often annual, seasonal, or ephemeral.

From a geomorphic perspective, a successful dynamic restoration project involves enhancement of aeolian activity (i.e., the entrainment, transport, erosion, and/or deposition of windblown sand) and dune morphodynamics, as well as periodic rejuvenation of landscape erosion-stabilization cycles, or 'dynamism' (Kooijman, 2004; Van Der Meulen *et al.*, 2004; Arens and Geelen, 2006; Nordstrom, 2008). In addition, re-establishment of nutrient-limited soil conditions coupled with wind erosion, abrasion, and sand burial associated with vegetation removal and enhanced aeolian activity favours early successional (pioneer) species over later successional species, which often form monocultures, to promote a more diverse, specialist dune plant community (Van Zoest, 1992; Kooijman, 2004; Arens and Geelen, 2006; Nordstrom, 2008). Together, these factors promote a more resilient dune ecosystem that holds greater ecological value than a stabilized system (Nordstrom, 2008).

Following the restoration treatment, the foredune at Wickaninnish had a lower, wider profile resulting from equipment activity and vegetation removal in September and, in the year following, showed appreciable and statistically significant volumetric recovery (+200 m^3) as did the landward transgressive dune system (+284 m^3). This resulted from the combined effects of reduced vegetation cover, which reduced sand trapping and wind drag effects thereby improving sand delivery from the beach (source)

to the transgressive dune complex (sink), and a significant influx of new sediment to the beach (834 m^3) that provided additional supply for landward transport.

In addition, geomorphic diversity and resilience have increased following the restoration treatment. Geomorphic resilience, which reflects the ability of the system to recover to some pre-disturbance state following a perturbation (Nordstrom, 2008) is evidenced by recovery of the dune profile to a form similar to that pre-restoration with additional progradation on the lower stoss and toe (~1 m) and extension of new depositional lobes into the lee (Figs. 6, 7, 9c, d). This is also confirmed by annual cross-shore profiles preceding and following the restoration activity (Fig. 10). Improved landform diversity, resilience and maintenance of natural erosion-recovery cycles are further demonstrated by the reactivation of the southeastern edge of the transgressive dune complex, new depositional lobes in the lee of the crest, re-establishment of the sand ramp to infill the eroded lower stoss slope, and recovery of the incipient dune zone fronting the foredune.

All of these findings suggest that this portion of the Wickaninnish Dunes complex has experienced enhanced aeolian activity, positive sediment volume changes, and improved geomorphic resilience over the first year following mechanical restoration. Should these responses continue, it is anticipated that dune mobility and active sand surface area within the study site would increase. Heathfield and Walker (2011) documented a 28% decline in active sand surface area within the larger foredune-transgressive dune complex between 1973 and 2007 and suggested that colonization by *Ammophila spp*. on the foredune and encroachment by native Kinnikinnik (*Arctostaphylos uva-ursi*) and Sitka spruce (*Picea sitchensis*) on the transgressive dune

perimeter were responsible. It has been documented that foredunes colonized by invasive *Ammophila* experience alterations in their sediment budgets that result in reduced landward sand transfers and dune steepening (e.g., Wiedemann and Pickart, 1996; Hesp, 2002). In contrast, foredunes vegetated with the native dune grass (*Leymus mollis*), which has a lower density growth pattern, tend to be less steep, more hummocky, and more dynamic geomorphically. Given regional climate trends toward wetter, warmer conditions (Walker and Sydneysmith 2008) and observed rates of dune stabilization, it is possible that without vegetation removal and enhance aeolian activity within this dune system complete stabilization of the transgressive dunes could occur within a few decades (Heathfield and Walker, 2011).

In terms of broader ecosystem restoration initiatives, PCA continues to monitor species recovery, maintains a manual pulling program for *Ammophila*, and is introducing the SARA-listed Pink sand verbena (*Abronia umbellate var breviflora*) in selected plots within the broader dune complex. To date, however, there is little information to assess species and ecological community responses to the restoration initiative, although this is part of the larger PCA project initiative.

2.7. Conclusions

This paper documented the novel case study of a dynamic dune restoration initiative that involved mechanical removal of invasive foredune vegetation to improve landscape dynamism. It provides an easily implemented, cost effective, and precise methodology that uses common surveying technologies and open-source software to provide an accurate and repeatable method for identifying significant geomorphic and sediment volume changes in dune landscapes. A geostatistical approach using kriging and

open-source software designed for geomorphic change detection in river systems (Wheaton et al. 2010) was used to model statistically significant changes within beach, foredune, and transgressive dune geomorphic units separately. This resulted in low average cross-validation error (0.0058 m) and the method provided a robust account for uncertainty in each DEM, with volumetric results (Table 3, Figure 7) consistent with other findings at the site (Figures 5, 8, 9). From these results, impacts on sediment volume changes and geomorphic responses to the restoration initiative were assessed.

Large-scale destabilization of the foredune had appreciable effects on the beach-dune system, shown through observed volumetric and geomorphic changes as follows:

1. The beach maintains a positive sediment volumetric change of 834 m^3 (0.187 m^3 m^{-2}), largely within the incipient dune zone. This provides a store of sediment available both as a buffer to wave attack and for further transport beyond the backshore,
2. Following the restoration treatment, the foredune profile was widened with increased sediment transported into the lee side of the foredune (200 m^3 or 0.128 m^3 m^{-2}), and
3. The transgressive dune complex receives additional sediment volume (+284 m^3 or 0.066 m^3 m^{-2}, largely via extension of depositional lobes from the foredune and accretion along the downwind edge of the dune complex.

Finally, the dynamic restoration treatment at the site was effective, in terms of increasing habitat for the SARA-listed Pink sandverbena (*Abronia umbellate var breviflora*) via promoting enhanced aeolian activity, improving geomorphic diversity, and increasing sediment exchanges between landscape units. These responses were not

observed in the control data; either prior to restoration at the study site or at a nearby site of similar geomorphology where vegetation removal was not complete. Ongoing monitoring of the study site will provide insights to the long-term sustainability of this emerging type of coastal dune restoration.

2.8. Acknowledgements

The author gratefully acknowledges field and research assistance from Hawley Beaugrand, Danielle Bellefleur, Mike Collyer, Derek Heathfield, and Nicholas von Wittgenstein. LiDAR and digital orthophotography was processed by Hawley Beaugrand in the Hyperspectral LiDAR Research Group lead by Dr. Olaf Niemann in the Department of Geography, University of Victoria. Partial travel funding and logistical support was provided by Parks Canada Agency, Pacific Rim National Park Reserve. Fieldwork and data analyses were funded by a Natural Sciences and Engineering Research Council (NSERC) Discovery Grant to I. Walker and a Geological Society of America research grant and NSERC Alexander Graham Bell Canadian Graduate Scholarship to J. Eamer.

3. Quantifying spatial and temporal trends in beach-dune volumetric changes using spatial statistics

3.1 Abstract

Spatial statistics are generally underutilized in geomorphology, despite offering great potential for identifying and quantifying spatial-temporal trends in landscapes and their formative processes. In particular, local Moran's I_i provides a statistical framework for identifying clusters of an attribute of interest (e.g., surface erosion or deposition) and quantifying how this attribute changes over space and time. This paper presents analysis of spatial-temporal patterns in sediment volume changes in a beach-foredune-transgressive dune complex following invasive marram grass (*Ammophila* spp.) removal. Vegetation was mechanically removed from a swath of foredune approximately 50 m wide in August 2009 as part of a dynamic restoration strategy at Wickaninnish Beach, British Columbia, Canada. Results are derived via comparison of post-removal landscape Digital Elevation Models (DEMs) derived from laser total station surveys (roughly every month) to a pre-restoration baseline control DEM obtained from an airborne LiDAR survey of the 10,320 m^2 study site. The baseline DEM was subtracted from subsequent DEMs using a basic pixel-subtraction algorithm and were filtered for statistically significant change. The filter was based on local Moran's I_i, which was used to generate 1.5m and 5m distance thresholds of statistically significant geomorphic change. These thresholds were specified to simulate the outer limit of saltating grains and the dimensions of landform development, respectively. Statistically significant volumetric change was mapped, calculated, and compared with volumetric change calculations based

on a simpler statistical threshold using the student's *t* distribution. Results show that spatial statistics were found to provide both more realistic calculated volumes at a smaller threshold distance and better highlighting of important spatial processes at a larger threshold distance than the volumetric change calculations based on a simpler statistical threshold.

3.2. Introduction

3.2.1. Context and research objectives

Coastal dunes store and cycle large amounts of sand and are key components of the coastal sediment budget (e.g., Short and Hesp, 1982; Hesp, 2002; Psuty, 2004). They provide an important 'buffer' of sediment along shorelines subject to extreme and/or increasing storm surge and erosion impacts and more gradual sea-level rise (e.g., Davidson-Arnott, 2005; Houser et al., 2008; Mascarenhas and Jayakumar, 2008; Eamer and Walker, 2010). On the Pacific coast of Canada, mixed sandy coastlines comprise less than 30% of the shoreline and less than 10% of this consists of dune-backed sandy beaches. Though rare, dune ecosystems are dynamic, sensitive and among the most threatened in Canada and they provide critical habitat for a plethora of endemic, migratory and endangered species. In British Columbia, there is recent interest to protect and restore these ecosystems under the federal Species At Risk Act (SARA) as there are dozens of species of concern that exist in sandy coastal ecosystems. New restoration efforts, such as the one with Parks Canada Agency that provides the opportunity for this study, have begun and research on dune morphodynamics and recovery to implemented treatments is foundational for these projects.

Geographic Information Systems (GIS) have been adopted broadly in geomorphology as a means to map, quantify and analyse spatial data across a range of scales, which is key to understanding landscape to landform scale responses in coastal systems (Andrews et al., 2002). For instance, the generation of Digital Elevation Models (DEMs) for sediment volumetric change analysis is commonly used to study the morphodynamics of beach-dune systems (e.g., Gares et al., 2006; Anthony et al., 2006). However, caution needs to be exercised in quantifying and interpreting volumetric changes and related geomorphic responses from DEMs given the uncertainties and errors associated with surveying and interpolation methods that affect DEM precision and accuracy. Recent research on dune morphological changes using DEMs (e.g., Woolard and Colby, 2002; Mitasova et al., 2005; Anthony et al., 2006; Reitz et al., 2010) implement different methodologies of data acquisition (e.g., Light Detection and Ranging (LiDAR), Real-Time Kinematic GPS (RTK-GPS), digital photogrammetry, laser total station surveys) and spatial interpolation modelling (e.g., Inverse Distance Weighted (IDW), Regularized Spline with Tension and Smoothing (RST), unspecified Kriging model). Critical to the accuracy of volumetric estimates and geomorphic patterns derived from DEM data is the consideration of uncertainty, which arises from survey point quality (e.g., instrument precision), sampling strategy (e.g., point spacing), surface composition (e.g., unconsolidated vs. consolidated surfaces), topographic complexity, and interpolation methods (Wheaton et al., 2010). Moreover, when differencing DEMs to calculate sediment volumetric changes, uncertainty is additive due to comparison of DEMs with their own individual uncertainty. Thus, the typical approach of using either a largely arbitrary minimum level of detection threshold based on unspecified empirical

determination (often 5 cm, e.g., Anthony et al., 2006) or no uncertainty in the results (e.g., Mitasova et al., 2005) obtained from DEM analysis, is insufficient. In the former, thresholds are not specific to the dat and may filter out small, but real, change. In the latter, reported volumetric changes may or may not be representative of actual change at the site because uncertainty and statistical significance are not considered in volumetric estimates.

Spatial statistics provide an alternative means for quantifying and interpreting geomorphic activity using DEMs. Recently, the application of Local Indicators of Spatial Association (or Autocorrelation)(LISA)(Anselin, 1995) has gained traction in the natural sciences as a statistical method for quantifying spatial patterns. In particular, LISA refers to a local measure of the Moran's I_i statistic, which can be used to distinguish positive and negative spatial autocorrelation (SA) based on the attribute value of a location in relation to the values of its neighbours (Nelson and Boots, 2008). A Moran's scatterplot (applicable to both global (discussed below) and local statistics) is a typical method of representing these relationships wherein the x-axis is the attribute value and the y the standardized average of the neighbour values (Anselin, 1995). Moran's scatterplots are separated into four quadrants where the upper right quadrant indicates a high value surrounded by other high values (HH), usually referred to as a "hot spot", the bottom left a low value surrounded by other low values (LL), or a "cold spot", the top left a low surrounded by high (LH), and the bottom right a high surrounded by low (HL). Typical application of local Moran's I_i in the natural sciences is to detect phenomenological hot and cold spots, or locations where something out of the ordinary, or extreme relative to the spatial mean, has occurred in one or more regions within the broader data field (Ord

and Getis, 2001). In geomorphic DEM analyses , hot spots would represent clusters of statistically significant deposition (Dh for deposition hotspot) and cold spots would indicate clusters of significant erosion (Ec for erosion coldspot). The other quadrants (HL and LH) typically represent outliers in the data whose importance varies based on the scope of the study and, using the geomorphology example, would simply represent outliers of deposition and erosion (Do and Eo), respectively.

There are three key benefits of incorporating spatial statistics into a geomorphic study. First, the investigation is statistically grounded, rather than largely observational or arbitrary. Second, the analyses are spatially guided, or based on the variation of an attribute of interest within a spatial neighbourhood. Third, the methods test a statistical null hypothesis that observed spatial patterns could have risen by chance, with rejection of the null hypothesis defining the threshold for hot spots (Nelson and Boots, 2008). Use of spatial autocorrelation methods in coastal geomorphology is generally lacking despite the potential for spatial statistics to provide new insight into underlying process-response relations in landscapes via computational pattern recognition.

Nelson and Boots (2008) discuss the implications of implementing local Moran's I_i in the presence of global SA. Whereas global measures (such as the Global Moran's I) look at each value in comparison to the complete dataset, local measures compare the value of a given observation with locations in that value's vicinity, thus providing a spatial component to results. . However, testing the significance of local SA is complicated by global SA and, as such, it is recommended that statistical tests associated with local measures be done in the presence of global SA be used in an exploratory manner, rather than as confirmatory statistical testing. Furthermore, the likelihood of

falsely identifying significant local SA increases in the presence of global SA (Ord and Getis, 2001).

The purpose of this paper is to apply local spatial autocorrelation statistics (local Moran's I_i) to identify and interpret statistically significant volumetric and geomorphic changes in a recently destabilized foredune-transgressive dune system in southwestern British Columbia, Canada. This study builds upon previous research by Section 2 that documented initial geomorphic responses at the study site using a student's *t* distribution for uncertainty estimation (using Geomorphic Change Detection software (Wheaton et al., 2010) and employs local Moran's I_i to identify different process-response patterns in the landscape by examining statistically significant responses at varying spatial scales that correspond to the aeolian transport process and larger landscape dynamics. Specific research objectives include:

1. To investigate the application of local Moran's I_i to DEMs derived from detailed topographic survey data collected in a coastal dune setting.

2. To quantify and describe significant volumetric changes and related geomorphic responses in the beach-dune complex following destabilization in comparison to the pre-restoration landscape.

3. To compare and contrast results generated using local Moran's I_i to those from the GCD approach presented by Section 2 in an effort to identify how spatial statistics can improve on the detection and analysis of significant geomorphic changes at varying spatial scales.

3.2.2. Regional Setting

The study area is located within the Wickaninnish Dunes complex within Pacific Rim National Park Reserve (PRNPR) on southwestern Vancouver Island near Ucluelet, British Columbia, Canada (Figure 1). The dune complex is located toward the southern end of a 10-km long embayed beach within Wickaninnish Bay, which has a southwest aspect to the Pacific Ocean, a mesotidal range (spring tide range ~4.2 m), and is exposed to energetic wave conditions (average winter significant wave height of 2.47 m and period 12.07 s). Beaches in the area are wide, dissipative and backed by 1 to 5 m high vegetated foredunes that are prograding at a rate of approximately 0.2 m a^{-1} (Heathfield and Walker, 2011) in response to regression of relative sea-level in response to crustal uplift along the Cascadia subduction zone (Mazzotti et al., 2008). The foredunes are backed by the largest active transgressive coastal dune complex on Vancouver Island.

The study region experiences an annual average air temperature of 12.8°C (1971-2000) and high year-round precipitation (3305.9 mm). Rainfall occurs, on average, on 202.7 days of the year with 52% falling from October through January and only 18% falling during the summer months (May through August). It experiences frequent WNW summer winds and strong SE winter storm winds (Eid et al., 1993; Beaugrand, 2010) (Figure 1). The alignment erosional blowouts and depositional lobes within the transgressive dune complex indicate a dominant transport vector from the WNW driven by (drier) summer wind events, despite a resultant sand transport potential vector from the south.

The dunes at this site support a number of native plant species, predominantly American dune (wildrye) grass (*Leymus mollis*), beach morning glory (*Convolvulus soldanella*), beach carrot (*Glehnia littoralis*), kinnickinnick (*Arctostaphylos uva-ursi*) and

yellow sand verbena (*Abronia latifolia*). Dominant species on the foredune, however, are the introduced American and European beach (marram) grasses (*Ammophila breviligulata* and *A. arenaria*, respectively). In the transgressive dunes, vegetation succession has lead to encroachment along the margins by kinnikinnick and Sitka spruce (*Picea sitchensis*) that, combined with expansion of the invasive marram landward of the foredune, has lead to a reduction in active sand surface by 28% within the Wickaninnish Dunes complex since 1973 (Heathfield and Walker, 2011).

A stretch of approximately 3 km of foredune was identified by Parks Canada Agency (PCA) in 2008 for mechanical removal of invasive *Ammophila* spp. to restore dynamic dune habitat. The first phase of removal occurred on 21 September 2009 with approximately 200 m of foredune cleared of vegetation in the study region (Figure 2). This study examines changes in sediment volumes and geomorphology within distinct geomorphic units (beach, foredune, transgressive dune) over the first year following vegetation removal at a study site with 10,320 m^2 of active sand surface and a perimeter of 924 m (Figure 11). The site consists of a small transgressive blowout complex encompassed on all landward boundaries by forest vegetation and fronted by 75 m of fully denuded foredune. The beach is approximately 100 metres wide at low tide and hosts a sparsely vegetated incipient dune seaward of the established foredune. Discussion of the fuller restoration initiative, its rationale, and the extent of vegetation removal is provided in Darke et al. (in review).

Figure 13. Map of the study area separated into discrete geomorphic units: beach, foredune and transgressive dune complex. The outer boundaries were defined by the outer limits of the survey with the smallest areal coverage. The inner boundaries (essentially bounding the shoreward and landward limits) of the foredune are defined in Section 2.

3.3. Methods

3.3.1. Data collection and DEM generation

Baseline topographic data were collected from airborne LiDAR flown on 27 August 2009 just prior to vegetation removal on the following 21 September. Point density of the LiDAR data was 1.13 pt m^{-2}, or roughly one point per metre, and a conservative estimate for vertical accuracy on bare sand is 15 cm. These data provide a control dataset against which subsequent laser total station surveys taken bi-monthly are

compared. Total station data have an instrument precision of 5 mm and an average point spacing of 0.06 pt m^{-2}, or roughly one point every 4 m (Section 2. DEMs were generated at 1 m grid cell resolution using the ordinary Kriging algorithm using the R statistical software packages geoR (Ribeiro and Diggle, 2001) and RGDAL (R Geospatial Data Abstraction Library). Differenced DEMs were generated by a simple pixel subtraction procedure: for a difference map at t_2, the elevation value at t_1 (LiDAR base-map) was subtracted from the elevation value at t_2, which generates snapshots of landscape change at t_2 relative to the initial pre-removal state. An uncertainty threshold was generated, ranging from ±0.0087m to 0.0590m, for removing pixels whose change values exceeded the precision of the experimental procedure. This threshold included survey closing error (obtained by surveying the same point at the beginning and end of the survey and noting vertical change), cross-validation (interpolation) error (documented in Section 2), and stated instrument precision (5 mm). These difference maps were then ready for application of a local Moran's I_i threshold for analysis of significant clusters of surface change.

3.3.2. Application of local Moran's I_i

Local Moran's I_i was implemented using GeoDa™ software, a freely available package developed by Anselin et al. (2006). After data import, spatial weights were generated using assigned threshold distances (TDs). Spatial weights provide the underlying control on spatial statistical analyses by limiting the neighbourhood over which spatial relationships are calculated and they are constructed with the data based on contiguity (for polygons) or distance (for point locations) thresholds (Anselin et al., 2006). There are two methods for determining spatial neighbourhoods for point locations:

i) TD, which considers all points falling within set distance from the analysis point, or ii) k-nearest neighbour, which considers the closest *k* number of point locations to the analysis point. TD is appropriate when data locations are regularly spaced and there is a theoretical reason for a specific distance being selected (Nelson and Boots, 2008). For this study, the regularity of the DEM pixels satisfied the former, while the latter was satisfied by choosing TDs of 1.5 m and 5 m to approximate the outer range for aeolian saltation transport distances and to reflect a scale comparable to dune form and spacing within the study area, respectively.

These spatial weights were then used in the local Moran's I_i analyses on each change map, using a maximum p-value of 0.05 (statistically significant to the 95^{th} percentile). Statistical significance for Moran's I is based on a random permutation procedure, which recalculates the statistic many times to generate a reference distribution (Anselin et al., 2006). In this study, the default 499 permutations were conducted. Values are then compared to the reference distribution to test the statistical hypothesis that surface change is not due to chance. Global statistics were also calculated (see section 3.1). Return values, or clusters of extreme values (Dh and Ec) and outliers (Do and Eo) of deposition and erosion, were exported to each shapefile and imported back into a GIS to generate maps of local Moran's I_i clusters and remove pixels from the original surface change DEMs that were not statistically significant. From this, volumetric changes for each surface change map and spatial weight (TD) were calculated.

3.4. Results

The results presented here span three stages of data analysis described above, including: i) global Moran's I statistics for each survey reported as suggested in Nelson

and Boots (2001)(section 3.1) as well as maps of clusters of significant deposition and erosion relative to the mean, ii) geomorphic change maps generated using defined spatial TDs for significant change detection (generated using local Moran's I_i) on surface change DEMs (section 3.2), and iii) volumetric change estimates for each geomorphic unit calculated from significant change DEMs (also provided in section 3.2).

3.4.1. Moran's I statistics and mapped clusters of deposition and erosion

In this study, the value of Moran's I was sufficiently high (i.e., > 0.6) and significant for both spatial thresholds to indicate global spatial autocorrelation (Table 4). Generally, the value of global Moran's I was reduced with increasing spatial weight (TD), even though the increased TD resulted in larger areas of significant surface change. In part, this relates to the notable increase in significant outliers, discussed below, that reduce the global SA. Although global spatial autocorrelation exists, using local Moran's I_i for threshold generation was considered warranted as the data generated by the local Moran's I_i wasn't used as an absolute measure of activity (i.e., instead being used for significance testing on pre-determined volumetric change).

Table 4. Global Moran's statistics for each change DEM dataset indicate the presence of global spatial autocorrelation.

	Global Moran's I Statistic	
Survey (Julian Day)	**1.5 m threshold distance**	**5 m threshold distance**
September 24 (267)	0.9134	0.7450
October 23 (296)	0.8978	0.6769
December 8 (342)	0.8940	0.6278
January 15 (15)	0.9080	0.6990
March 5 (64)	0.9428	0.7611
April 13 (103)	0.9139	0.7374
May 30 (150)	0.9381	0.7590
July 8 (189)	0.9070	0.7447
August 14 (226)	0.8994	0.7324

(Annual total)		

Five of the nine interval datasets (23 Oct., 5 Mar., 13 Apr., 30 May, 14 Aug.) are mapped in Figures 12-15 below for ease of interpretation and to explore seasonal variations in morphodynamics response within the dune complex (see also Section 2). Note that the August survey represents an annual time period, as survey dates refer to a snapshot of beach-dune evolution relative to the initial LiDAR survey in August 2009. Maps of clusters of extreme deposition and erosion relative to the mean (and outlier values) are shown for the 1.5 m TD (Figure 13) and the 5m TD (Figure 14), and surface coverage areas of local Moran's I_i clusters for each TD are shown in Table 5.

Table 5. Areal coverage of each result of local Moran's I_i analyses, where Dh is deposition hotspot, Do is deposition outlier, Eo is erosion outlier, and Ec is erosion coldspot.

	Area of each local Moran's I_i indicator (m^2)							
	1.5 m threshold distance				**5 m threshold distance**			
Survey (Julian Day)	**Dh**	**Do**	**Eo**	**Ec**	**Dh**	**Do**	**Eo**	**Ec**
September 24 (267)	2177	15	4	2302	3185	319	187	3389
October 23 (296)	1461	12	11	1799	2505	450	130	3859
December 8 (342)	1894	19	23	1411	2552	422	365	3355
January 15 (15)	1896	2	16	1913	3967	107	517	2181
March 5 (64)	2846	7	12	2477	5135	70	491	2752
April 13 (103)	2344	10	0	2112	3406	366	152	3567
May 30 (150)	2890	6	6	2913	4260	171	226	3626
July 8 (189)	1942	12	5	1982	3083	373	224	3540
August 14 (226) (Annual total)	2100	6	8	1582	2980	369	314	3551

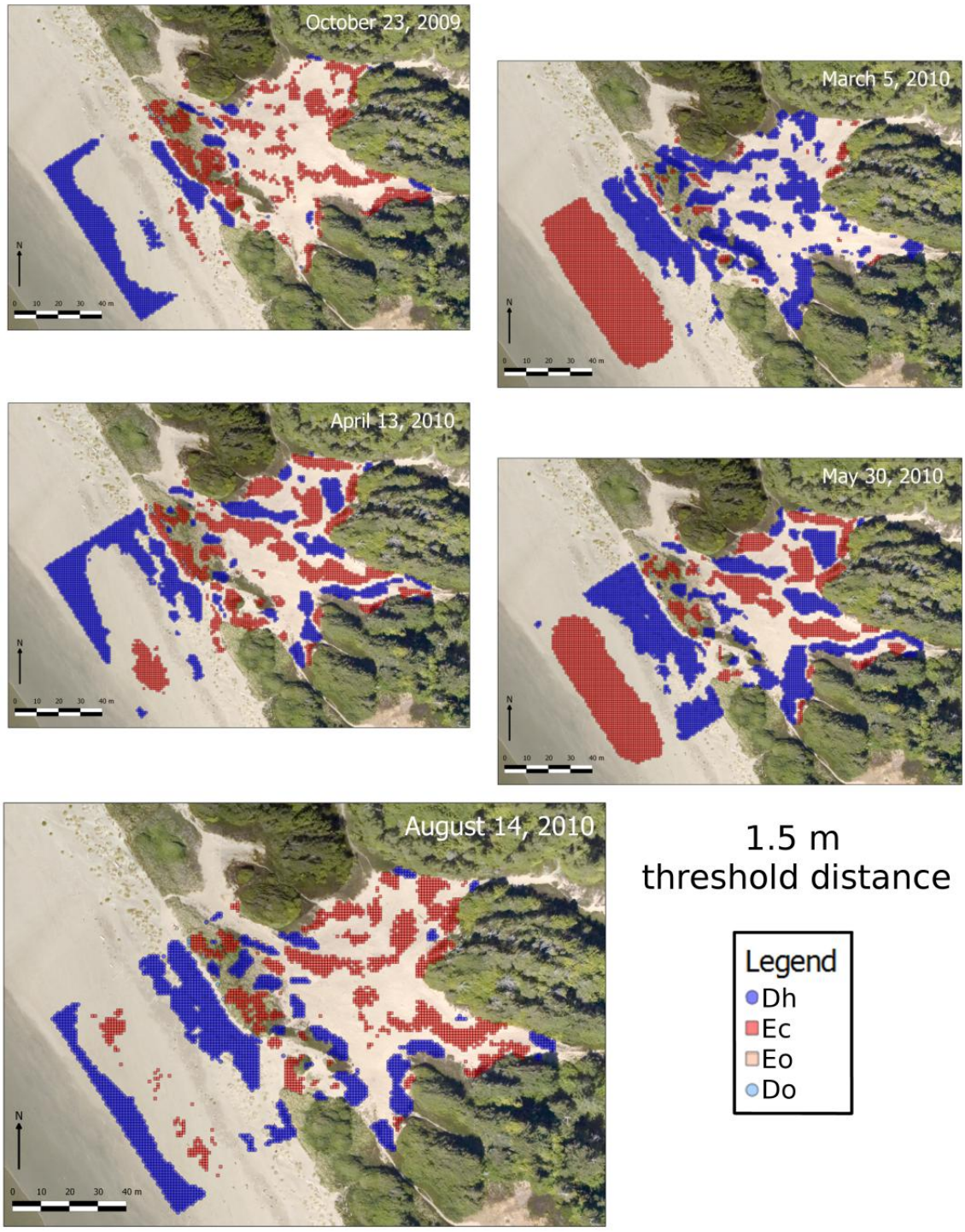

Figure 14. Select maps of local Moran's I_i -generated clusters of significant surface change for the study site. Survey date shown in the upper right corner of each map. These maps were generated using a 1.5m TD spatial weight.

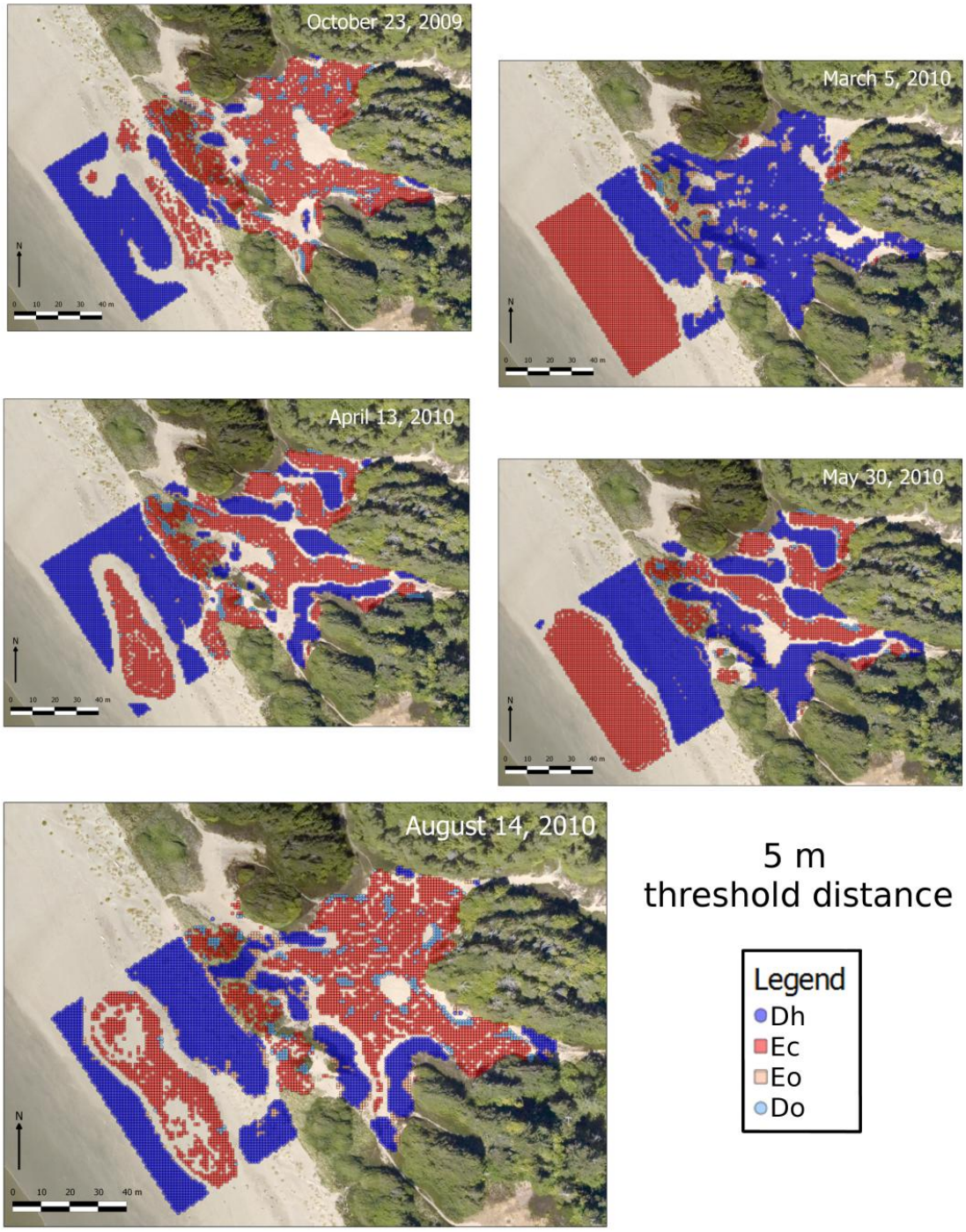

Figure 15. Select maps of local Moran's I_i -generated clusters of significant surface change for the study site. Survey date shown in the upper right corner of each map. These maps were generated using a 5m TD spatial weight.

The local Moran's I_i maps for the 1.5 m TD spatial weight (Figure 13) generally have very little outlier areal coverage and most of the study area is classified as clusters of Dh or Eh. Erosion dominates in the beach the winter and spring months (i.e., between October and May) and clusters of deposition build on the upper beach in the incipient dune zone during this time. Also, between March and May, Ec dominate the foredune stoss and Dh develop in the foredune lee. These depositional clusters continue to build through August. The transgressive dune complex shows the most variability with Ec dominating in October then replaced by Dh by March (with Eo), and linear clusters of Dh and Ec developing in subsequent surveys (largely aligned with the dominant transporting wind direction, from WNW). The surface area of Ec is generally greater than Dh (Table 5) except for December, March, and April.

The maps of local Moran's I_i derived using the 5 m TD spatial weight reveal an increase the surface area of all significant clusters of change (on average ~70%), with the outlier values increasing by an order of magnitude (e.g., for the annual Aug-Aug survey, an increase from 14 to 683 m^2). Generally, the spatial trends described above for the 1.5 m TD are continued and expanded, and patterns are smoothed out. The presence of Do and Eo is more evident in Figure 14 where they occur dominantly in the upper beach, foredune, and transgressive dune complex with fewer sporadic occurrences in the lower beach face. Again, the surface area of Eo is greater than that of Do, except for January, March, and May (when beach erosion dominates). Note also that the area of Dh clusters is nearly double that of the Eh clusters for March, the largest discrepancy for the dataset.

3.4.2. Geomorphic and sediment volume changes

Figures 14 and 15 are based on the original change DEMs for each geomorphic unit (using basic pixel subtraction described in section 2.1) with application of the 1.5 m and 5 m TD local Moran's I_i surfaces to filter out insignificant pixels. Corresponding values of volumetric changes in each geomorphic unit for each spatial weight TD are also provided in Table 6.

Table 6. Estimates of statistically significant sediment volume changes using spatial statistical thresholds. Area normalized values (in brackets) provide an effective depth of average sediment accretion (+) or erosion (-) within each unit.

	Volumetric change from LiDAR baseline (m^3) and area-normalized (m^3 m^{-2})					
	1.5 m threshold distance			**5 m threshold distance**		
Survey (Julian Day)	Beach: 4470 m^2	Foredune: 1565 m^2	Transgressive Dune: 4285 m^2	Beach: 4470 m^2	Foredune: 1565 m^2	Transgressive Dune: 4285 m^2
September 24 (267)	+572 (+0.128)	-59 (-0.012)	+61 (+0.014)	+746 (+0.167)	-31 (-0.020)	+187 (+0.044)
October 23 (296)	+647 (+0.145)	+11 (+0.065)	-39 (-0.009)	+956 (+0.214)	+45 (+0.029)	+155 (+0.036)
December 8 (342)	+322 (+0.072)	+80 (+0.088)	+97 (+0.019)	+483 (+0.108)	+127 (+0.081)	+221 (+0.052)
January 15 (15)	-162 (-0.036)	+82 (+0.058)	+145 (+0.034)	-133 (-0.030)	+124 (+0.079)	+302 (+0.071)
March 5 (64)	-635 (-0.142)	+136 (+0.072)	+242 (+0.057)	-650 (-0.145)	+159 (+0.102)	+368 (+0.086)
April 13 (103)	+523 (+0.117)	-17 (-0.062)	+132 (+0.031)	+766 (+0.171)	+31 (+0.020)	+270 (+0.063)
May 30 (150)	+232 (+0.052)	+64 (+0.082)	+228 (+0.053)	+365 (+0.082)	+116 (+0.074)	+348 (+0.081)
July 8 (189)	+627 (+0.140)	+35 (+0.091)	+8 (+0.002)	+870 (+0.195)	+198 (+0.127)	+112 (+0.026)
August 14 (226) (Annual total)	+611 (+0.137)	+100 (+0.128)	+66 (+0.015)	+863 (+0.193)	+162 (+0.104)	+287 (+0.067)

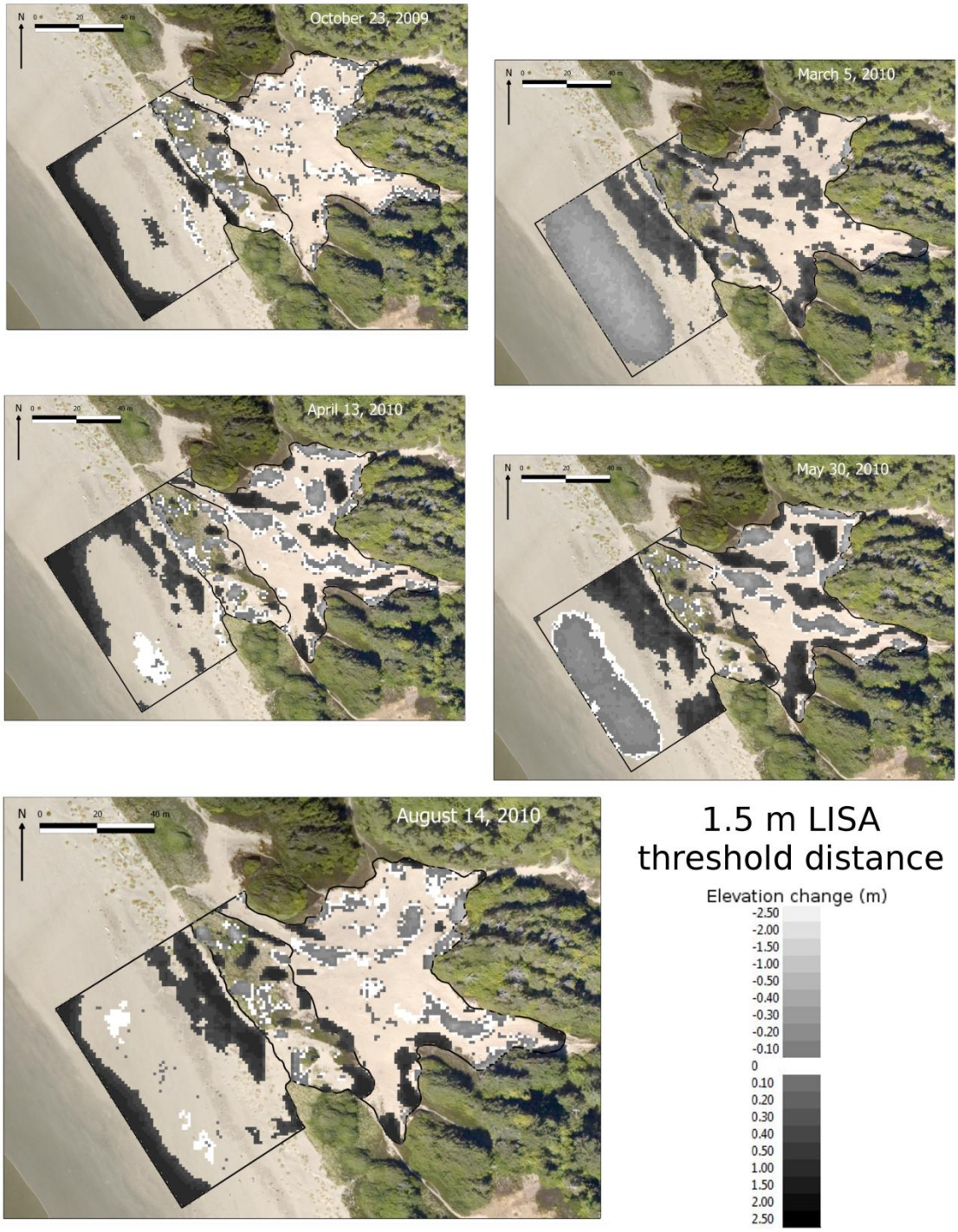

Figure 16. Select geomorphic change maps of the study area, with the survey date shown in the upper right corner of each map. These maps generated after applying the 1.5m TD local Moran's I_i statistics as a significant change threshold.

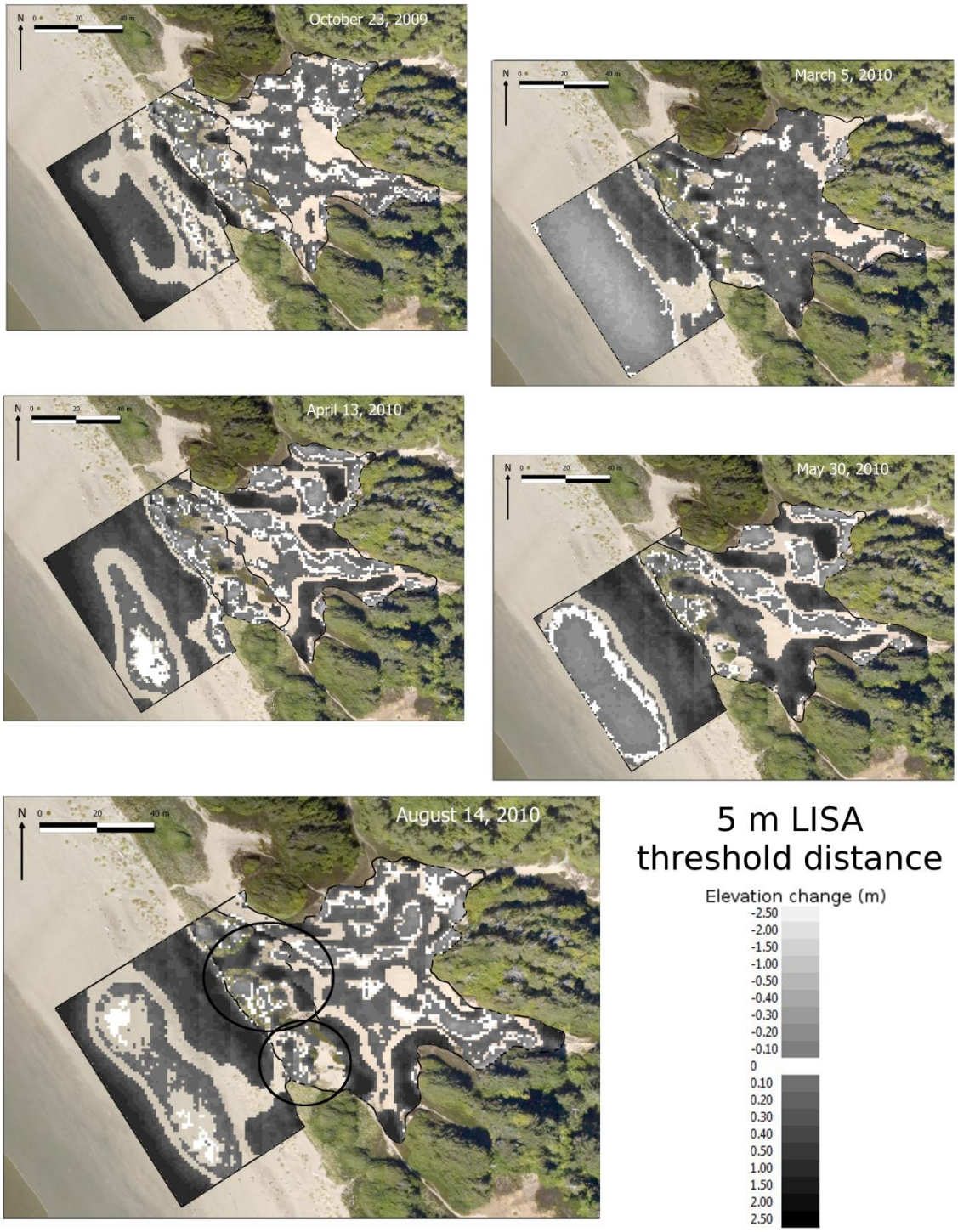

Figure 17. Select geomorphic change maps of the study area, with the survey date shown in the upper right corner of each map. These maps generated after applying the 5m TD local Moran's I_i statistics as a significant change threshold. Circles on the annual (August) change map indicate areas of interest discussed in section 3.5.3.

Annually, both the 1.5 m and 5 m TD spatial weights yielded net increases in sediment volume of +777 m^3 and +1313 m^3, respectively (note that the order of presenting results for each TD remains constant below) , and normalizing this by surface area yielded an effective depth of sediment accretion, which was +0.280 m^3m^{-2} and +0.368 m^3m^{-2}. Most of this accretion was in the beach unit (+0.137 m^3 m^{-2} and +0.193 m^3 m^{-2}), which was localized in the upper beach and incipient dune zone. In addition, lobes of deposition in the lee side of the foredune and downwind of the dominant transport vector (from WNW) into the transgressive dune complex account for the positive sediment volumes observed there (Table 6).

In addition to experiencing the highest amount of accretion annually, the beach surface exhibited the greatest total volumetric change (a general proxy for geomorphic activity) for both TDs (1282 m^3 and 1606 m^3 between the minimum and maximum points, October and March). Erosion and beach steepening began between December and January surveys and a low in the sediment volume (-635 m^3 and -650 m^3) was experienced by March, and the onset of summer wave conditions and transporting wind events (recall the inferred summer wind regime dominance discussed in 1.2) resulted in accretion after March. Most of the accretion was localized in the upper beach/incipient dune zone, aided by aeolian sediment transport off the beachface and seasonal vegetation growth in this area.

The foredune unit experienced deflation immediately after vegetation removal with the 1.5m TD volumetric response (-59 m^3) exceeding that of the 5m TD (-31 m^3). Recovery was slow with accretion in the lee side of the foredune initially offset by a stoss side scarp (see March and April change maps, Figures 14 and 15) to the extent that the

1.5m TD sediment volume change was negative by April (-17 m^3). As with the upper beach, the return to a positive sediment volume change coincided with the initiation of the summer wind regime and associated aeolian transport off the beachface (Table 6).

Landward of the foredune, the transgressive dune experienced the least volumetric change (Table 6). A decline in sediment volume occurs between the September and October surveys (resulting in a negative volume relative to the LiDAR survey of -39 m^3 for the 1.5m TD), however a mostly regular increase in sediment volume follows until the May survey. Between the May and July surveys, 220 m^3 (1.5m TD) and 236 m^3 (5m TD) are denuded from the transgressive dune complex. Sediment volumes recover marginally for the annual (August) surveys.

3.5. Discussion

3.5.1. Interpretation of local Moran's I_i results and their geomorphic relevance

Using the local Moran's I_i statistics in an exploratory manner reveals a number of patterns across the study area. First, as discussed in Section 1.1, an intuitive interpretation of the HH and LL clusters produced by Moran's I_i for this study are clusters of extreme deposition and erosion (Dh and Ec), respectively (Figs. 11, 12). However, when interpreted this way, the difference between the October and March 5m TD local Moran's I_i maps indicate a notable shift from an erosive transgressive dune complex to a depositional one. However, when the same interval is presented as the 5m TD geomorphic change DEMs (Fig. 16), no such overall change is observable. This can be explained by the extent of the vertical change data in each map. The beach surface reflects a steeper winter profile by March with a highly denuded beach face. This area of

denudation is absent in the October survey, when a less steep summer beach profile is still remnant. Thus, in March, there is a much lower "low" point in the elevation change data, drawing the distribution of data downward, forcing the data in the transgressive dune complex into a "depositional" setting, relative to the mean of the March data. Thus care must be taken in interpreting local Moran's I_i results, and, in the case of this study, are more useful as both exploratory statistics and as an intermediary step (such as statistical threshold testing, which would be largely unaffected by a distribution shift).

Implementation of local Moran's I_i can be useful in exploratory analysis due to the flexibility in exploring various spatial scales of analysis. For instance, in this study two different spatial weights (TDs) were applied to identify statistically significant responses at two different spatial scales a very local (1.5m) threshold that scales with the saltation process and a larger landform scale (5m). A researcher could examine broader (landscape) scales by implementing a larger threshold distance, or more specific spatial scales with knowledge of the modal dimensions of various processes or landforms of interest. As in Table 5, the 1.5m TD in this study resulted in a "buffering" of extreme results (i.e., Eh and Dh were less extensive), which can be explained by the smaller spatial neighbourhood (and thus smaller sample size) utilized to calculate the statistic. From a geomorphic perspective, however, this may relate to the smaller TD (1.5m) only producing locally significant changes, more directly a result of a migrating depositional lobe (see the lee side of the foredune, May and August, Figure 15), rather than broad scale (5m TD) landform change (note how these lobes are, for the most part, integrated into broader depositional areas, Figure 16).

Recall that depositional and erosional outliers as defined by local Moran's I_i (Do and Eo) represent anomalies in otherwise smooth patterns across the study site. These become more evident in Fig. 14, with the higher TD, as more outliers are revealed. This is a result of the increased spatial neighbourhood (and thus amount of data) included in each statistical test. Outliers are predominantly depositional (with the exception of the March survey, when outliers are largely erosional for reasons described above). The distribution of outliers is focused in the foredune and transgressive dune and likely represents localized areas of deposition around sparse vegetation in these areas. In particular, yellow sand verbena (*Abronia latifolia*) and sea rocket (*Cakile edentula*) (Fig. 17) provide low, sparse roughness to produce more uniform Do clusters (e.g., those in the foredune). Also, big-head sedge (*Carex macrocephala*)(Fig. 18), which has trailing rhizomes that often align linearly and stabilize trailing ridges of dunes in the transgressive dune complex, may be responsible for the elongated Do clusters. Thus local Moran's I_i may provide a good first order remotely sensed estimate of the vegetation characteristics of a study site.

Figure 18. Picture taken in August 2010 of the back of the transgressive dune complex, showing the deflation area upwind of the precipitation ridge, with two yellow sand verbena plants in the foreground. Note the localized deposition around each plant.

Figure 19. Picture taken in August 2010 of a blowout in the transgressive dune complex with the trailing rhizomes of a big-head sedge plant located behind the researcher. Note the linear localized accretion surrounding the vegetation-anchored sediment (similar to the trailing arm of a parabolic dune).

3.5.2. Geomorphic responses within the beach-dune system

Figure 19 provides a graphical summary of the data provided in Table 5, as well as the results of analyses using GCD (section 1.1) from Section 2 for comparison in the following section 4.3. High amounts of variability in beach volume reflect the varying contributions of and interactions between wave- and wind-driven sediment transport processes. Accretion in the lower beach face and the incipient dune zone were the drivers for the increased volume seen under both TDs, however, the increase is buffered with the 1.5m TD (+647m^3) when compared with the 5m TD (+946 m^3), the result of factors

discussed in Section 4.1. The two different TDs agreed well through the erosional period (October through April) due to the extreme nature of the changes and the spatial contrast allowing for straightforward identification of significant change (i.e., erosional change values are extreme relative to the mean). Beach recovery was hindered by the migration of a rip cell embayment through the study area in May, which steepened the beach profile and resulted in a net loss of 291 m^3 and 401 m^3 of sediment from the beach for the 1.5m and 5m TDs, respectively. Subsequent beach recovery resulted in sediment volumes that are not much greater than those surveyed in April (Fig. 19), however the distribution of sediment changed from swash deposited sediments in the lower beach to aeolian deposited sediments in the upper beach/incipient dune zone (Figs. 13, 14).

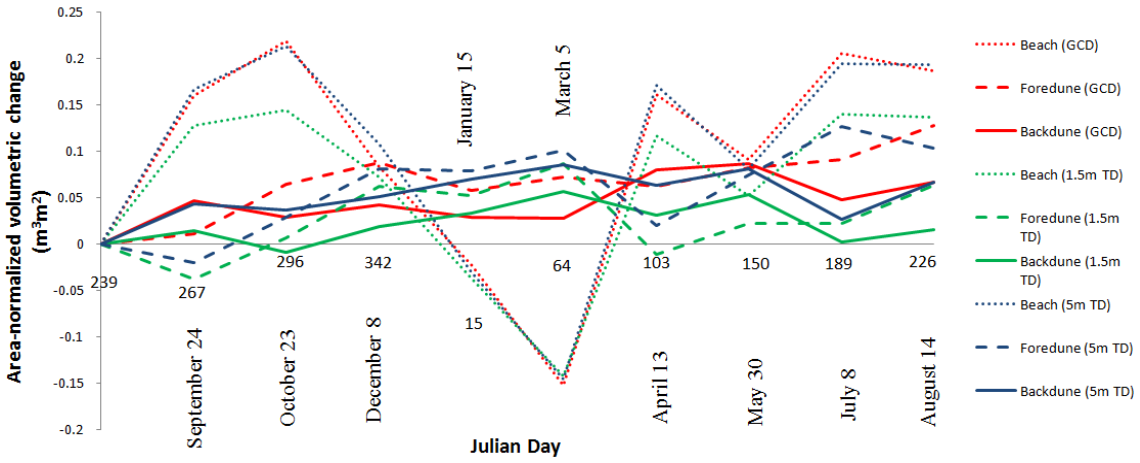

Figure 20. Volumetric change time series in the dune system after the initial LiDAR survey for each geomorphic unit. Note the values from the two TD spatial weights generated in this study and the values from the GCD analysis approach from Section 2.

Deflation in the foredune following vegetation removal was largely attributed to the coincident removal of sediment during the mechanical restoration procedure. Deposition in the foredune crest and lee contributed to the positive sediment volumes

observed through March (+136 m^3 and +159m^3 for the 1.5m and 5m TD, respectively), even when the foredune stoss and toe were extensively deflated and scarped (Figs. 15 and 16) due to high water events and storm activity through late fall and winter. However, between the March and April surveys, storm activity removed an appreciable amount of sediment, with the 1.5m TD yielding a negative and the 5m TD yielding a small positive sediment volume (Table 5). Again, as with the beach, surface deflation was modeled similarly between the two TDs while deposition is buffered in the 1.5m TD (resulting in the negative sediment volume for the April survey). This difference can be attributed to: i) the more marked surface change under erosive conditions being detectable for both TDs while gradual aeolian buildup went undetected by the smaller threshold distance, and/or ii) wave eroded surfaces generally being flatter (and less likely to be lost in interpolation) compared to more hummocky aeolian depositional surfaces. Finally, aeolian rebuilding occurred after April, with sediment transport into the stoss and lee of the foredune (+117 m^3 and +131 m^3 deposited between April and August for each TD) allowing for scarp recovery and transport over the foredune into depositional lobes. The upper circle located on the foredune in Figure 16 indicates a conduit for sediment transport on and through the foredune into the transgressive dune (Figure 20). This was observed in the 5m TD change maps, but less so in the 1.5m TD change map and is discussed further in Section 4.3. The lower circle highlights erosion on the stoss side of a kremholtz Sitka that was not removed in August 2009 (Figure 21).

Figure 21. Sand sheet creating a transport pathway through the foredune at the study site. Photo taken August 2010. Location highlighted as the NW-most yellow circle in Fig. 16
.

Figure 22. Photo at the study site showing: i) deflation at the foredune toe in front of the tree island, visible by the coarser, darker sediment located in the depression, and ii) accretion in the upwind (i.e., left) side of the tree island, visible by the Sitka Spruce die-off due to burial. Photo taken August 2010 with the location indicated by the SE-most yellow circle in Fig. 16.

Initial accretion in the transgressive dune complex is offset by deflation by October (-100 m^3 and -32 m^3 for the 1.5 and 5m TDs, respectively), which, given appropriate lag time following deflation of the foredune (Figure 19), could be due to a loss of available sediment for landward transport, exhibiting the coupling between these two units. Alternating erosional and depositional phases (with a gradual trend of accretion) occur between January and May (Table 5, Fig. 19), with the patterns organizing into upwind (toward WNW) deflation feeding downwind accretion. The same

lagged deflation pattern discussed above emerges between the April and July surveys, where deflation of the foredune (-153 m^3 and -128 m^3 for each TD between March and April) results in later deflation in the transgressive dune complex (-220 m^3 and -236 m^3 for each TD between May and July). Final accretion of the transgressive dune complex occurs predominantly as sediment begins to bypass the foredune, with i) a transport conduit at the north end of the foredune allowing deposition on the landward side of the transgressive dune complex, ii) sediment accreting on the eastern edge of the dune complex, fed sediment from the reworking of upwind well developed depositional lobes in the lee side of the foredune, and iii) deposition on a transgressing arm in the eastern-most portion of the dune complex. All this contributes to a modest +66 m^3 and +287 m^3 of accretion for the 1.5m and 5m TDs, respectively, over the full year of data. Again, the 1.5m TD is preferential to erosion in the transgressive dune complex (Figures 14 and 15), with little of the broad pattern of deposition that was observable in the 5m TD.

3.5.3. Comparison of local Moran's I_i generated geomorphic change thresholds and those using GCD

Section 2 present an account of the evolution of this coastal dune system, using the same source data and similar geomorphic maps and volumetric calculations based on DEM analyses using GCD software. Thresholds generated in that study were based on a statistical student's *t*-test using methodological uncertainties, and they were applied uniformly over the study area for each DEM. In contrast, thresholds in this study were applied on a local basis, with each pixel values evaluated for significance in a defined region of values.

Figure 19 shows the volumetric change for each geomorphic unit over the study period for each TD from this study and the volumetric change from Section 2. In the beach, the volumetric change over the full year rarely differs between the GCD and 5m TD results, with a the greatest separation between the two datasets occurring in December (0.03 m^3 m^{-2}). The 1.5m TD data, however, exhibit the deposition-controlled "buffer" discussed above, where negative (erosional) sediment volumes are modeled similarly at the expense of muted response when both the GCD and 5m TD results show highly positive sediment volumes (e.g., 0.09 m^3 m^{-2} separating the 1.5m TD volume from other results on the October survey (Figure 19)). The maps (Figures 6, 14, and 15) all show similar cycles of erosion and deposition, with the areal extent of upper beach accretion being more similar between the 5m TD and GCD methods. At the beach-dune interface, however, there are more marked differences between the local Moran's I_i and GCD methods. The deep scarp at the foredune toe, confirmed by photographic evidence in Section 2, is more pronounced and further landward into the stoss of the foredune at both TDs.

In the foredune, deflation immediately following vegetation removal, as expected by sediment removal associated with *Ammophila* removal, is detected by both local Moran's I_i TDs, but not by the GCD method. Afterwards, rapid recovery of the foredune follows until March, with both TDs reaching sediment volumes of +0.02 m^3 m^{-2} and+0.04 m^3 m^{-2} above GCD values for 1.5m and 5m, respectively. The erosion of the foredune between the March and April surveys, prevalent in the Moran's I_i results (discussed above), is minimal in the GCD results (-16 m^3 between the two surveys). This is largely due to the foredune scarp remaining largely unfilled in the local Moran's I_i volumetric

change maps, while nearly gone in the GCD volumetric change maps. Finally, photographic evidence of features largely undetected by the GCD method show a sediment transport conduit through the foredune, outlined by the northernmost circle in Figure 16, which was discussed above (Figure 20). Directly observed in the field, this feature accreted sediment across the stoss and crest of the foredune, with appreciable amounts of sediment being deposited as lee-side depositional lobes. Neither the GCD nor 1.5m TD maps convey this feature exhibited in Figure 20, while the 5m TD does. Figure 21, outlined by the southernmost circle in Figure 16, shows the erosion on the stoss side of a kremholtz Sitka that was not removed in August 2009. Both the 1.5m and 5m TD capture this erosion; however the GCD method does not.

In the transgressive dune, the volumetric trends of the 1.5m and 5m TDs is almost identical, however the 1.5m TD consistently shows 0.3 to 0.5 m^3 m^{-2} less volumetric change relative to the LiDAR survey. Both patterns and values are nearly identical between the 5m TD and GCD results, with one distinction being between the months of December and March. The March change map for the 5m TD (Figure 16) exemplifies this difference as being one already discussed in Section 5.1. The lowering of the distribution of data for the 5m TD in January and March due to beach steepening and erosion lead to more surface change at the study site being extreme relative to the mean, and thus more significant change was detected than was probably warranted. Thus the absence of significant volumetric change in the transgressive dune complex observed in the GCD results is likely more true to the actual volumetric change at the site.

It would appear that the two different spatial thresholds serve two different and correspondingly useful functions. The 1.5m TD indicates a more conservative (related to

both the 5m TD and GCD methods) estimate of volumetric change at the site, with less of the detrimental data distribution effects discussed in section 4.1. Annual volume changes are more realistic in a beach dune system that has undergone one year of change following vegetation removal: foredune sediment volumes became negative after both mechanical and wave-driven denudation, and annual transgressive dune complex volume change increased more modestly (after what was likely an erosional or net-zero sediment volume change prior to restoration, given the likelihood of very low sediment input over an *Ammophila* dominated dune). Recall that this spatial scale was utilized to simulate the outer spatial limit of saltating grains. Thus using the 1.5m TD as a significance threshold for sediment transport, and thus volumetric transfers over the beach-dune system, appears more attractive for volumetric estimates than the 5m TD or the GCD method.

In addition, the 5m TD was ideal for feature identification in concurrent data analyses. Sedimentological features that were confirmed with field reconnaissance, such as the foredune transport conduit and the erosional hollow (that may develop into a foredune blowout), were identified in the 5m TD change map (Figure 16). As the 5m TD was generated to simulate landform development, it provided a useful threshold for detecting spatially continuous features developed across the study site that remained undetected in the 1.5m TD or GCD change maps.

3.6. Conclusions

This paper explored the use of spatial statistics for quantifying and examining volumetric changes and geomorphic response in coastal dune systems using high-resolution DEMs. The goal of this research was to investigate the properties of spatial statistics, namely local Moran's I_i, and how these statistics can be applied to surface

change maps generated from DEMs. The use of local Moran's I_i for generating surface change results is attractive: they are statistical in nature, they look at a local spatial neighbourhood surrounding the value under investigation, and significance is inferred upon rejection of the null hypothesis (i.e., complete spatial randomness). In addition, the methodology is repeatable, cost-effective, and user friendly, based on freely-available open source software. Using different TDs, surface change maps were generated using local Moran's I_i that identified clusters of statistically significant surface change, and these maps were used to calculate volumetric change in a coastal system following a dynamic restoration strategy. The local Moran's I_i statistics were also useful in investigating the first order vegetative properties of the study site. When compared to a DEM analysis using GCD (significance based on the student's *t* distribution) using the same source data, spatial statistics were found to provide both more realistic calculated volumes at a smaller threshold distance and better highlighting of important spatial processes at a larger threshold distance not uncovered by the GCD-generated change DEMs. When properly specified, using spatial statistics for threshold generation provides a robust, quantitative account of both volumetric change and sedimentological activity in coastal geomorphology, two important proxies for determining the state of a coastal system.

3.7. Acknowledgements

The author gratefully acknowledges field and research assistance from Hawley Beaugrand, Danielle Bellefleur, Mike Collyer, Derek Heathfield, and Nicholas von Wittgenstein. LiDAR and digital orthophotography was processed by Hawley Beaugrand in the Hyperspectral LiDAR Research Group lead by Dr. Olaf Niemann in the

Department of Geography, University of Victoria. Partial travel funding and logistical support was provided by Parks Canada Agency, Pacific Rim National Park Reserve. Fieldwork and data analyses were funded by a Natural Sciences and Engineering Research Council (NSERC) Discovery Grant to I. Walker, a Geological Society of America research grant and NSERC Alexander Graham Bell Canadian Graduate Scholarship to J. Eamer.

4. Conclusion

4.1. Summary and conclusions

This thesis provides new methodologies for accurately quantifying geomorphic change in a coastal setting. The study utilizes data typical to coastal geomorphology (e.g., total station, LiDAR) obtained from August 2009 through August 2010 and manipulate it using easily implemented, cost effective, and repeatable processes. Results were used to quantify volumetric and surficial change in a discrete coastal system following devegetation of the foredune, a novel approach to coastal dune restoration. This thesis is structured around two results sections (2 and 3) derived from data collected between August of 2009 and 2010 at a beach-dune system located in the Wickaninnish Dunes, Pacific Rim National Park Reserve, British Columbia, Canada. Each section is prepared as a manuscript to be submitted for publication in a peer-reviewed journal. Section 2 documented the novel case study of a dynamic dune restoration initiative that involved mechanical removal of invasive foredune vegetation to improve landscape dynamism. Section 3 explored the use of spatial statistics for quantifying and examining the same volumetric change data, with the stated goal of providing improved estimates of volumetric and surficial change. These sections are bookended with an Introduction (Section 1) that sets the research context and this section that reviews key findings of the research.

The purpose of Section 2 was to refine a methodology for identifying multi-temporal and multi-spatial geomorphic changes between and over all geomorphic units at the study site and assess the effectiveness of the implemented treatment (dynamic dune

restoration) for increasing dune activity. A geostatistical approach using kriging and open-source software designed for geomorphic change detection in river systems (Wheaton et al. 2010) was used to model statistically significant changes within beach, foredune, and transgressive dune geomorphic units separately. This resulted in low average cross-validation error (0.0058 m) and the method provided a robust account for uncertainty in each DEM. It was found that the beach maintained a positive sediment volumetric change of 834 m^3 (0.187 $m^3\,m^{-2}$), largely within the incipient dune zone. This provided a store of sediment available both as a buffer to wave attack and for further transport beyond the backshore. In addition, the foredune profile was widened with increased sediment transported into the lee side of the foredune (200 m^3 or 0.128 $m^3\,m^{-2}$). Finally, the transgressive dune complex received additional sediment volume (+284 m^3 or 0.066 $m^3\,m^{-2}$, largely via extension of depositional lobes from the foredune and accretion along the downwind edge of the dune complex.

Finally, the dynamic restoration treatment at the site was effective, in terms of increasing habitat for the SARA-listed Pink sandverbena (*Abronia umbellate var breviflora*) via promoting enhanced aeolian activity, improving geomorphic diversity, and increasing sediment exchanges between landscape units. These responses were not observed in the control data; either prior to restoration at the study site or at a nearby site of similar geomorphology where vegetation removal was not complete.

Section 3 utilizes tools provided by the field of spatial statistics, namely local Moran's I_i, to assess statistically significant patterns and change at the study site using the same dataset from Section 2. The purpose of this section was to investigate the applicability of local Moran's I_i as applied to DEMs in a coastal setting by comparing this

method to the conventional approach of Section 2. Using different TDs, surface change maps were generated using local Moran's I_i that identified clusters of statistically significant surface change, and these maps were used to calculate volumetric change in a coastal system following a dynamic restoration strategy. The local Moran's I_i statistics were also useful in investigating the first order vegetative properties of the study site. When compared to a DEM analysis using GCD (significance based on the student's *t* distribution) using the same source data, spatial statistics were found to provide both more realistic calculated volumes at a smaller threshold distance and better highlighting of important spatial processes at a larger threshold distance not uncovered by the GCD-generated change DEMs.

4.2. Research contributions and future directions

The major contribution of this research is the development of new methodologies for determining volumetric and surficial changes in a coastal system in an accurate and repeatable manner. As discussed above, previous work on meso-scale coastal dune studies inadequately addresses methodological concerns such as interpolation statistics and quantification of error, and as such the comparison and synthesis of studies in the field suffers. Through the expansion of a geostatistical framework provided by Swales (2002), and application of GCD (section 2) and local Moran's I_i (section 3) techniques to data documenting a coastal dune restoration, a statistical basis for error estimation was created. Comparison of the two methodologies revealed GCD as an ideal simple approach to geomorphic mapping and error estimation, with local Moran's I_i providing more customizable and (given proper utilization) accurate estimates of volumetric change and surficial properties at the study site. As the properties of local Moran's I_i were

specifically designed for application to this study site, further use in sites of differing morphologic conditions will provide more insight into the benefits of such an analysis.

In addition to the methodological role, the documenting of a large scale dynamic dune restoration (a first of its kind in Canada) provides an important contribution to the coastal geomorphology literature. Increased aeolian activity, geomorphic diversity, and sediment exchanges across the beach-dune system were observed in both sections 2 and 3, and these factors combine to provide more habitat for the target species. Thus, restoration success can be inferred based on these factors, however long term monitoring and maintenance (e.g., manual marram grass removal) are recommended. Also, the effects of vegetation removal on the foredune resulted in what can be considered an intuitive morphodynamic response: removal of the surface roughness provided by vegetation and aeolian sediment transfers were less hindered. Further use of data used in this study can perhaps be beneficial to development of meso-scale process-response modeling. Finally, recommendations for future coastal dune management scenarios are as such:

1. Coastal restoration projects are inherently multidisciplinary, and require inputs from many facets of science (e.g., ecology, geomorphology, GIS),
2. A strong monitoring program, with baseline control data and long-term support, is highly beneficial to directing efforts and achieving mandates, and
3. If restoring for active sand surface habitat, the most ideal location for re-introduction of threatened species is the lee-side of a fully de-vegetated foredune. This should be adjusted for the burial tolerance of each species.

5. References

Agterberg FP. 2004. Georges Matheron: Founder of Spatial Statistics. Earth Sciences History **23**: 205-334.

Andrews BD, Gares PA, Colby, JD. 2002. Techniques for GIS modeling of coastal dunes. Geomorphology **48**: 289-308.

Anselin L. 1995. Local Indicators of Spatial Association-LISA. Geographical analysis **27:** 93-114.

Anselin L, Syabri I, Kho Y. 2006. GeoDa: An introduction to spatial data analysis. Geographical Analysis **38:** 5-22.

Anthony EJ, Vanhee S, Ruz M. 2006. Short-term beach-dune sand budgets on the north sea coast of France: Sand supply from shoreface to dunes, and the role of wind and fetch. Geomorphology **81**: 316-329.

Anthony EJ, Vanhee S, Ruz M. 2007. An assessment of the impact of experimental brushwood fences on foredune sand accumulation based on digital elevation models. Ecological Engineering **31**: 41-46.

Arens SM. 1997. Transport rates and volume changes in a coastal foredune on a Dutch Wadden Island. Journal of Coastal Conservation **3**: 49-56.

Arens SM, Slings Q, de Vries CN. 2004. Mobility of a remobilized parabolic dune in Kennemerland, The Netherlands. Geomorphology **59**: 175-188.

Arens B, Geelen L, Slings R, Wondergem H. 2005. Restoration of dune mobility in the Netherlands. In: Herrier JL, Mees J, Salman A, Seys J, Van Nieuwenhuyse H, Dobbelaere I. (Eds.), Proceedings 'Dunes and Estuaries 2005' – International Conference on Nature Restoration Practices in European Coastal Habitats, Koksijde, Belgium, 19-23.

Arens SM and Geelen LHWT. 2006. Dune landscape rejuvenation by intended destabilization in the Amsterdam water supply dunes. Journal of Coastal Research **22**: 1094-1107.

Baas ACW. 2002. Chaos, fractals and self-organization in coastal geomorphology: simulating dune landscapes in vegetated environments. Geomorphology **48** : 309-328.

Baas ACW, Sherman DJ. 2006. Spatiotemporal variability of aeolian sand transport in a coastal dune environment. Journal of Coastal Research **22**: 1198 – 1205.

Bauer, B., Sherman, D., 1999. Coastal dune dynamics: problem and prospects. In: Goudre, A.S., Livingston, I., Stokes, J. (Eds.), *Aeolian Environments, Sediments and Landforms*. London: J. Wiley and Sons Ltd.

Bauer BO, Davidson-Arnott RGD, Hesp PA, Namikas SL, Ollerhead, J, and Walker IJ. 2009. Aeolian sediment transport conditions on a beach: Surface moisture, wind fetch, and mean transport rates. Geomorphology **105**: 106-116.

Beaugrand HER. 2010. Beach-dune morphodynamics and climate variability impacts on Wickaninnish Beach, Pacific Rim National Park Reserve, British Columbia, Canada. Unpublished MSc Thesis, University of Victoria, Canada.

Brock JC, Wright CW, Sallenger AH, Krabill WB, Swift RN. 2002. Basis and Methods of NASA Airborne Topographic Mapper Lidar Surveys for Coastal Studies. Journal of Coastal Research **18**: 1-13.

Bruun P. 1954. Coast Erosion and the Development of Beach Profiles. Beach Erosion Board Technical Memorandum 44, Washington DC: US Army Corps of Engineers, 79p.

Bruun,P. 1962. Sea level rise as a cause of shore erosion. Journal of Waterways and Harbors Division, ASCE, **88**: 117-130.

Chapman C, Walker IJ, Hesp PA, Bauer BO, Davidson-Arnott RGD, Ollerhead JO. (in review). Turbulent Reynolds stress distributions and sand transport responses over a vegetated foredune. Earth Surface Processes and Landforms.

Chappell A, McTainsh G, Leys J, Strong C. 2003. Using geostatistics to elucidate temporal change in the spatial variation of aeolian sediment transport. Earth Surface Processes and Landforms **28**: 567-585.

Christiansen MB, Davidson-Arnott, RGD. 2004. Rates of landward sand transport over the foredune at Skallingen, Denmark and the role of dune ramps. Danish Journal of Geography **104**: 31-43.

D'Antonio C. and Meyerson LA. 2002. Exotic plant species as problems and solutions in ecological restoration: a sythesis. Restoration Ecology **10**: 703-713.

Darke IB, Davidson-Arnott RG, Ollerhead J. 2009. Measurement of beach surface moisture using surface brightness. Journal of Coastal Research **25**: 248 – 256.

Darke IB, Walker IJ. 2010. Coastal Geoindicators Monitoring for Climate Change and Coastal Erosion in Pacific Rim NPR. Report PR-2010-03, Winter 2010.

Darke IB, Walker IJ, Eamer JBR. In review. Geomorphical Considerations for Dynamic Dune Restoration: Pacific Rim National Park Reserve, British Colombia, Canada. Earth Surface Processes and Landforms.

Davidson-Arnott RGD. 2005. Conceptual model of the effects of sea level rise on sandy coasts. Journal of Coastal Research **21**: 1166-1172.

Davidson-Arnott RGD, MacQuarrie K, Aagaard T. 2005. The effect of wind gusts, moisture content and fetch length on sand transport on a beach. Geomorphology **68**: 115-129.

Davidson-Arnott RGD, Bauer BO, Walker IJ, Hesp PA, Ollerhead J, and Delgado-Fernandez I. 2009. Instantaneous and mean aeolian sediment transport rate on beaches: An intercomparison of measurements from two sensor types. Journal of Coastal Research **SI56**: 297-301.

Debruyn W, Deronde B, Fransaer D, Henriet J, Houthuys R, Lancker VV. 2006. Use of Airborne Hyperspectral Data and Laserscan Data to Study Beach Morphodynamics along the Belgian Coast. Journal of Coastal Research **22:** 1108-1117.

Delgado-Fernandez I, Davidson-Arnott R, Ollerhead J. 2009. Application of a remote sensing technique to the study of coastal dunes. Journal of Coastal Research **25**: 1160 – 1167.

Delgado-Femandez I, Davidson-Arnott RGD. 2011. Meso-scale aeolian sediment input to coastal dunes: The nature of aeolian transport events. Geomorphology **126**: 217-232.

Eamer JBR, Walker IJ. 2010. Quantifying sand storage capacity of large woody debris on beaches using LIDAR. Geomorphology **118**: 33-47.

Eid B, Calnan C, Henschel M, McGrath B, 1993. Wind and wave climate atlas: Volume IV the West Coast of Canada. Montreal, Quebec, Canada: Transport Canada. Retrieved 16 May 2011 from http://www.meds-sdmm.dfo-mpo.gc.ca/alphapro/wave/TDCAtlas/tdcatlaswc.htm

Englund E. and Sparks A. 1991. Geostatistical Environmental Assessment Software GEO-EAS 1.2.1 Users Guide. Las Vegas, Nevada: Environmental Monitoring Systems Laboratory, United States Environmental Protection Agency, 130p.

Gares PA, Wang Y, White SA. 2006. Using LIDAR to monitor a beach nourishment project at Wrightsville Beach, North Carolina, USA. Journal of Coastal Research **22**: 1206-1219.

Gornitz V. 1995. Sea-level rise: a review of recent past and near-future trends. Earth Surface Processes and Landforms **20**: 7-20.

Grootjans AP, Geelen HWT, Jansen AJM, Lammerts EJ. 2002. Restoration of coastal dune slacks in the Netherlands. Hydrobiologia **478**: 181-203.

Heathfield DK, Walker IJ. 2011. Analysis of coastal dune dynamics, shoreline position, and large woody debris at Wickaninnish Bay, Pacific Rim National Park, British Columbia. Canadian Journal of Earth Sciences **48**: 1185-1198.

Hesp PA. 2001. The beach backshore and beyond. In: Short, A.D. (Ed.), Handbook of Beach and Shoreface Morphodynamics. Wiley, London, pp. 145-169.

Hesp PA. 2002. Foredunes and blowouts: initiation, geomorphology and dynamics. Geomorphology **48**: 245-268.

Hesp PA, Davidson-Arnott R, Walker IJ, Ollerhead J. 2005. Flow dynamics over a foredune at Prince Edward Island, Canada. Geomorphology **65** : 71-84.

Houser C, Hapke C, Hamilton S. 2008. Controls on coastal dune morphology, shoreline erosion and barrier island response to extreme storms. Geomorphology **100**: 223-240.

Houser C, Hamilton S. 2009. Sensitivity of post-hurricane beach and dune recovery to event frequency. Earth Surface Processes and Landforms **34** : 613 – 628.

Houser, C. 2009. Synchronization of transport and supply in beach-dune interaction. Progress in Physical Geography **33**, 733-746.

Jackson DWT, Beyers JHM, Lynch K, Cooper JAG, Baas ACW, Delgado-Fernandez I. 2011. Investigation of three-dimensional wind flow behaviour over coastal dune morphology under offshore winds using computational fluid dynamics (CFD) and ultrasonic anemometry. Earth Surface Processes and Landforms, **36**: 1113-1124.

Jensen JL, Lake LW, Corbett PWM, Goggin DJ. 1997. Statistics for Petroleum Engineers and Geoscientists. Upper Saddle River, NJ: Prentice Hall, 390p.

Kollmann J, Brink-Jensen K, Frandsen SI, Hansen MK. 2011. Uprooting and burial of invasive alien plants: a new tool in coastal restoration? Restoration Ecology **19**: 371 – 378.

Krige DG. 1951. A statistical approach to some mine valuations and allied problems at the Witwatersrand. Master's thesis, University of Witwatersrand.

Lee DS and Shan J. 2003. Combining LIDAR elevation data and IKONOS multispectral imagery for coastal classification mapping. Marine Geodesy **26:** 117-127.

Liu X. 2008. Airborne LiDAR for DEM generation: some critical issues. Progress in Physical Geography **32:** 31-49.

Lynch K, Jackson DWT, Cooper JAG. 2008. Aeolian fetch distance and secondary airfl ow effects: the infl uence of micro-scale variables on meso-scale foredune development Earth Surface Processes and Landforms **33**: 991–1005. DOI:

Mascarenhas A and Jayakumar S. 2008. An environmental perspective of the post-tsunami scenario along the coast of Tamil Nadu, India: role of sand dunes and forests. Journal of Environmental Management **89**: 24-34.

Mazzotti S, Jones C, Thomson RE. 2008. Relative and absolute sea level rise in western Canada and northwestern United States from a combined tide gauge-GPS analysis. Journal of Geophysical Research **113**: 1-19.

Mitasova H, Overton M, Harmon RS. 2005. Geospatial analysis of a coastal sand dune field evolution: Jockey's Ridge, North Carolina. Geomorphology **72**: 204 – 221.

Nelson TA, Boots B. 2008. Detecting spatial hot spots in landscape ecology. Ecography **31:** 556-566.

Nickling WG and Davidson-Arnott RGD. 1990. Aeolian sediment transport on beaches and coastal sand dunes. In: Davidson-Arnott, R.G.D. (Ed.), *Proceedings of the Symposium on Coastal Sand Dunes.* Ottawa: National Research Council of Canada, pp. 1-35.

Nordstrom KF. 1990. The concept of intrinsic value in depositional coastal landforms. Geographical Review **80**: 68-81.

Nordstrom KF. 2008. Beach and Dune Restoration. Cambridge, England: Cambridge University Press, 187p.

Ord JK, Getis A. 2001. Testing for local spatial autocorrelation in the presence of global autocorrelation. Journal of Regional Science **41**: 411-432.

O'Sullivan D, Unwin DJ. 2003. Geographic Information Analysis. New York: Wiley, 436p.

Psuty NP. 1988. Sediment budget and dune/beach interaction. Journal of Coastal Research, **SI 3**: 1-4.

Psuty N. 1992. Spatial variation in coastal foredune development. In; Carter, R.W.G., Curtis, T.G.F., Sheehy-Skeffington, M.J. (Eds.), Coastal Dunes:

Geomorphology, Ecology, and Management for Conservation. Balkema, Rotterdam, pp.3-13.

Psuty N. 2004. The coastal foredune: a morphological basis for regional coastal dune development. In: Martinez ML and Psuty N (eds.), *Coastal Dunes, Ecology and Conservation*. New York, NY, Springer, pp. 11-27.

Reitz MD, Jerolmack DJ, Ewing RC, Martin RL. 2010. Barchan-parabolic dune pattern transition from vegetation stability threshold. Geophysical research letters 37, 5p.

Ribeiro JR, Diggle PJ. 2001. geoR: A package for geostatistical analysis. R-NEWS 1: ISSN 1609-3631.

Riksen M and Goossens D. 2005. Tillage techniques to reactivate aeolian erosion on inland drift-sand. Soil and Tillage Research **83**: 218-236.

Riksen M, Ketner-Oostra R, Van Turnohout C, Nijssen M, Goossens D, Jungerious PD, Spaan W. 2006. Will we lose the last active inland drift sands of Western Europe? The origin and development of the inland drift-sand ecotype in the Netherlands. Landscape Ecology **21** : 431-447.

Rozé F and Lemauviel S. 2004. Sand dune restoration in North Brittany, France: a 10-year monitoring program. Restoration Ecology **12**: 29-35.

Sallenger, Jr. AH, Krabill WB, Swift RN, Brock J, List J, Hansen M, Holman RA, Manizade S, Sontag J, Meredith A, Morgan K, Yunkel JK, Frederick EB,

Stockdon H. 2003. Evaluation of Airborne Topographic LIDAR for Quantifying Beach Changes. Journal of Coastal Research **19**: 125-133.

Saye, S., Vanderwal, D., Pye, K., and Blott, S. (2005). Beach-dune morphological relationships and erosion/accretion: An investigation at five sites in England and Wales using LIDAR data. Geomorphology **72**: 128-155.

Sherman DJ, Bauer BO. 1993. Dynamics of beach-dune systems. Progress in Physical Geography **17**: 413-447.

Sherman DJ. 1995. Problems of scale in the modeling and interpretation of coastal dunes. Marine Geology **124**: 339-349.

Short AD, Hesp PA. 1982. Wave, beach and dune interactions in Southeastern Australia. Marine Geology **48**: 259-284.

Swales A. 2002. Geostatistical estimation of short-term changes in beach morphology and sand budget. Journal of Coastal Research **18**: 338-351.

Unwin DJ. 1975. An introduction to trend surface analysis. *Concepts and Techniques in Modern Geography*. Geo Abstracts Ltd: University of East Anglia, Norwich, 40p.

van Boxel JH, Jungerius PD, Kieffer N, Hampele N. 1997. Ecological effects of reactivation of artificially stabilized blowouts in coastal dunes. Journal of Coastal Conservation **3**: 57-62.

van Hook SS. 1985. European beachgrass. Fremontia **12:** 20-21.

Walker IJ, Beaugrand HER. 2008. Coastal Geoindicators Monitoring-Protocol for Climate Change and Coastal Erosion in Canada's Pacific Coastal National Parks. Unpublished report submitted to Pacific Rim National Park Reserve, Ucluelet, BC. 39p.

Walker IJ, Hesp PA, Davidson-Arnott RGD, and Ollerhead J. 2006. Topographic steering of alongshore airflow over a vegetated foredune: Greenwich Dunes, Prince Edward Island, Canada. Journal of Coastal Research **22**: 1278-1291.

Walker IJ, Hesp PA, Davidson-Arnott RGD, Bauer BO, Namikas SL, Ollerhead J. 2009a. Responses of three-dimensional flow variations in the angle of incident wind and profile form of dunes: Greenwich Dunes, Prince Edward Island, Canada. Geomorphology **105**: 127-138.

Walker IJ, Davidson-Arnott RGD, Hesp PA, Bauer BO, Ollerhead J. 2009b. Mean flow and turbulence responses in airflow over foredunes: New insights from recent research. Journal of Coastal Research **SI56**: 366-370.

Wheaton JM, Brasington J, Darby SE, Sear DA. 2010. Accounting for uncertainty in DEMs from repeat topographic surveys: improved sediment budgets. Earth Surface Processes and Landforms **35**: 136-156.

Wiedemann AM, Pickart A. 1996. The Ammophila problem on the Northwest Coast of North America. Landscape and Urban Planning **34**: 287 – 299.

Wolfe SA, Walker IJ, Huntley DJ. 2008. Holocene coastal reconstruction, Naikoon peninsula, Queen Charlotte Islands, British Columbia. Geological Survey of Canada, Current Research 2008-12, 16p.

Woolard JW, Colby JD. 2002. Spatial characterization, resolution, and volumetric change of coastal dunes using airborne LIDAR: Cape Hatteras, North Carolina. Geomorphology **48**: 269-287.

Zhang K, Witman D, Leatherman S, Robertson W. 2005. Quantification of beach changes caused by Hurricane Floyd along Florida's Atlantic coast using airborne laser surveys. Journal of Coastal Research **21**: 123-134.